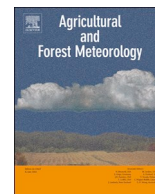




ELSEVIER

Contents lists available at ScienceDirect

## Agricultural and Forest Meteorology

journal homepage: [www.elsevier.com/locate/agrformet](http://www.elsevier.com/locate/agrformet)Energy and CO<sub>2</sub> exchange in an undisturbed spruce forest and clear-cut in the Southern TaigaVadim Mamkin<sup>a,\*</sup>, Julia Kurbatova<sup>a</sup>, Vitaly Avilov<sup>a</sup>, Dmitry Ivanov<sup>a</sup>, Olga Kuricheva<sup>a</sup>, Andrej Varlagin<sup>a</sup>, Irina Yaseneva<sup>b</sup>, Alexander Olchev<sup>a,b</sup><sup>a</sup> A.N. Severtsov Institute of Ecology and Evolution, Russian Academy of Sciences, Leninskiy Prosp. 33, 119071, Moscow, Russia<sup>b</sup> Faculty of Geography, Lomonosov Moscow State University, GSP-1, Leninskie Gory, 119991, Moscow, Russia

## ARTICLE INFO

## Keywords:

Clear-cut  
Undisturbed boreal forest  
Southern taiga  
Energy fluxes  
CO<sub>2</sub> fluxes  
Eddy covariance

## ABSTRACT

Effects of clear cutting and other forest disturbances on surface radiative properties and the energy and CO<sub>2</sub> fluxes between land surface and the atmosphere can vary significantly depending on local climatic and moisture conditions, forest structure and species composition, soil properties and many other factors. In this study we analyzed the influence of clear-cutting on the energy, water vapor and CO<sub>2</sub> fluxes in the still very poorly investigated part of the boreal forest community in the European part of Russia. This issue has become particularly relevant due to intensified logging in the region during recent decades. The sensible ( $H$ ) and latent ( $LE$ ) heat, as well as CO<sub>2</sub> fluxes were continuously measured at recently clear-cut and undisturbed mature spruce forest sites using eddy covariance technique during the first growing season following harvest. Because of their close location they are characterized by similar meteorological conditions. The results of our field measurements showed that the clear-cut strongly influenced the energy balance and CO<sub>2</sub> fluxes between the land surface and atmosphere. Energy fluxes ( $LE$  and  $H$ ) at the undisturbed forest site were consistently larger than at the clear-cut throughout the period of measurements. The Bowen ratio ( $\beta = H/LE$ ) varied significantly over time, though was similar at both sites. Whereas  $H$  was almost equal to  $LE$  at both sites in spring, the  $LE$  significantly exceeded  $H$  over the summer ( $\beta \approx 0.2$  - for mature spruce forest and  $\beta = 0.4$  - for clear-cut). The mean  $\beta$  for the entire period was similar ( $\beta \approx 0.5$ ) at both sites. Analysis of CO<sub>2</sub> fluxes showed that the clear-cut was a consistent source of CO<sub>2</sub> to the atmosphere. Net ecosystem exchange ( $NEE$ ) at the clear-cut averaged  $3.3 \pm 1.3 \text{ gC}\cdot\text{m}^{-2}\cdot\text{d}^{-1}$  ( $\pm 1 \text{ SD}$ ), while average  $NEE$  at the undisturbed mature forest was close to zero ( $0.1 \pm 1.9 \text{ gC}\cdot\text{m}^{-2}\cdot\text{d}^{-1}$ ). Differences in  $NEE$  were mainly governed by differences in gross primary productivity ( $GPP$ ) between sites ( $7.0 \pm 4.1 \text{ gC}\cdot\text{m}^{-2}\cdot\text{d}^{-1}$  and  $4.1 \pm 3.0 \text{ gC}\cdot\text{m}^{-2}\cdot\text{d}^{-1}$ , for the undisturbed forest and clear-cut, respectively). Total ecosystem respiration ( $TER$ ) did not significantly ( $p < 0.05$ ) differ between sites ( $7.1 \pm 3.6 \text{ gC}\cdot\text{m}^{-2}\cdot\text{d}^{-1}$  at the undisturbed mature forest and  $7.4 \pm 3.4 \text{ gC}\cdot\text{m}^{-2}\cdot\text{d}^{-1}$  at clear-cut).  $TER$  at the undisturbed forest showed higher sensitivity to changes in soil temperature, whereas  $GPP$  at the clear-cut was characterized by higher light-use efficiency. Our measurements showed that  $TER$  rates were relatively high in the southern taiga in comparison with other boreal sites where CO<sub>2</sub> fluxes were previously investigated.

## 1. Introduction

Boreal forests cover large areas in the northern hemisphere and have significant impacts on the climate system (Chen and Luo, 2015; Helbig et al., 2017; IPCC, 2013). Natural and anthropogenic forest disturbances can influence surface albedo, net radiation, sensible and latent heat, and CO<sub>2</sub> fluxes between the land surface and atmosphere, and can thus substantially affect climate conditions from local to global scales (Kulmala et al., 2014; Seidl et al., 2014). Effects of clear-cutting as a widespread logging practice on microclimatic conditions and

green-house gas (GHG) exchange nowadays are key topics of numerous experimental and modeling studies (Amiro et al., 2010; Grant et al., 2010; Keenan and Kimmins, 1993; Kowalski et al., 2003; McCaughey, 1985; Paul-Limoges et al., 2015; Radler et al., 2010; Sundqvist et al., 2014; Williams et al., 2014). As shown by McCaughey (1985), tree felling changes surface albedo and the amount of solar radiation that is absorbed, which leads to a corresponding increase in surface daytime temperatures. Furthermore, aggregated experimental and modeling studies showed that the size of the clear-cut can influence spatial patterns of radiation, wind, air and soil temperature both within and

\* Corresponding author.

E-mail addresses: [vadimmamkin@gmail.com](mailto:vadimmamkin@gmail.com), [vadimmamkin@sevin.ru](mailto:vadimmamkin@sevin.ru) (V. Mamkin).<https://doi.org/10.1016/j.agrformet.2018.11.018>

Received 23 April 2018; Received in revised form 11 November 2018; Accepted 19 November 2018

Available online 28 November 2018

0168-1923/ © 2018 Elsevier B.V. All rights reserved.

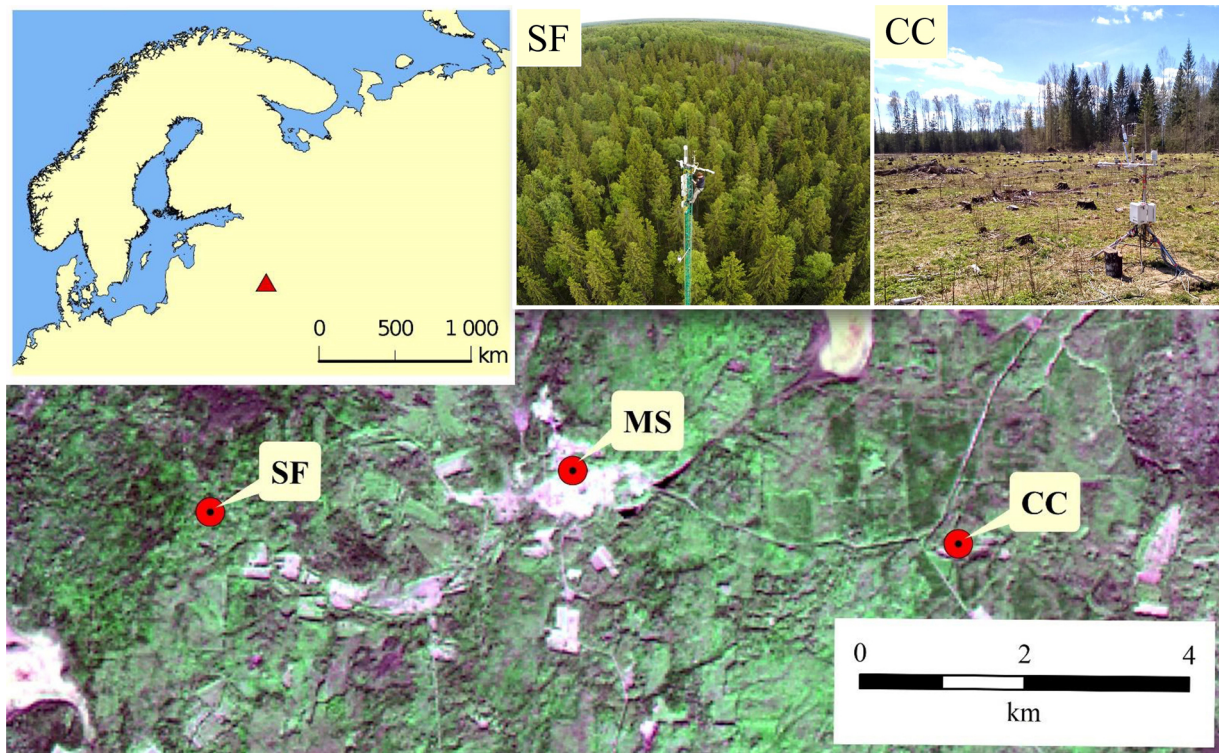


Fig. 1. Geographical location of the measurement sites (Landsat 8 image 23.03.2016). MS - meteorological station “Zapovednik”, SF – undisturbed mature spruce forest, CC – the clear-cut area.

outside the forest clearing (Carlson and Groot, 1997; Panferov and Sogachev, 2008; Olchev et al., 2009; Radler et al., 2010). All these factors affect the soil moisture and plant transpiration of clear-cuts and, as a result, the evapotranspiration of recently disturbed sites is generally lower than of undisturbed old-growth forests (Kowalski et al., 2003; Williams et al., 2014). As shown by Amiro (2001), clear cutting can decrease net radiation ( $R_n$ ), sensible ( $H$ ) and latent heat ( $LE$ ) fluxes, as well as increase the daily amplitude of soil heat flux ( $G$ ) during early succession in comparison with undisturbed mature forest ecosystems.

Most studies describing effects of forest disturbances on carbon budgets indicate that harvest can cause forest ecosystems to switch from a carbon sink to a carbon source for years to decades following disturbance (Amiro et al., 2010; Aguilos et al., 2014; Schulze et al., 2000; Zha et al., 2009). Vegetation regeneration in forest clearings leads to increasing  $CO_2$  uptake, the rate of which is depends on local weather, climate, vegetation and soil conditions. Bergeron et al. (2008) showed that the annual carbon budget of boreal forests in North America is more affected by the age of forest stands rather than by the variability of climatic parameters, and recently harvested sites have much larger inter-annual changes in their carbon budgets due to their plant species composition, structure and physiology. An analysis based on measurements from 28 eddy covariance stations in USA and Canada performed by Amiro et al. (2010) showed that most disturbed forest ecosystems became a sink within 20 years following harvest, but the  $CO_2$  fluxes substantially varied depending on geographical location of the clear-cut sites. A modelling study focused on the  $CO_2$  balance of larch forests in Hokkaido, Japan, concluded that clear cutting can influence the carbon balance even 52 years following harvest (Hirata et al., 2014). Most of these studies also found that  $CO_2$  emission outweighed uptake mainly because of reduced gross primary production ( $GPP$ ) following harvest rather than an increase in total ecosystem respiration ( $TER$ ).  $TER$  is usually similar pre- and post-harvest because the reduction in autotrophic respiration is compensated by the increase in heterotrophic respiration drive by the intensive decomposition of logging residues (Paul-Limoges et al., 2015). The factors controlling the

$CO_2$  net balance in young, fast-growing forests may greatly differ from those in mature and old growth forests (Humphreys et al., 2006). Studies also indicate that  $CO_2$  fluxes at mature and disturbed forest sites can significantly differ over time. The measurements provided by Coursolle et al. (2012) showed in particular that  $CO_2$  uptake and emission in young forest stands in Canada are strongly dependent on leaf area index ( $LAI$ ) and ambient weather conditions, whereas fluxes in mature forests dependent mostly on atmospheric parameters.

Numerous studies have focused on  $NEE$  of  $CO_2$  following forest disturbance in North America; however, there are large parts of the world (including Europe) where such information is still very limited (Matthews et al., 2017). Hirata et al. (2014) point to the need and importance of new flux data, especially from under-studied regions, to evaluate the potential diversity of responses of forest ecosystems to anthropogenic disturbances.

Boreal forests and temperate forests cover large areas in Russia and they play an important role in global carbon cycle, absorbing 200–500 million tones of  $CO_2$  every year primarily through forest management activities (FAO, 2011; Zamolodchikov et al., 2017). Since 2008 a steady decrease of carbon sink by Russian forests was observed. As found by Zamolodchikov et al. (2017), this reduction was caused mostly by logging (44.5%), fires (21.5%), and decreasing  $CO_2$  uptake (34.5%). The clear-cut areas in Russia have increased drastically from ~0.684 million hectares per year in 2001–2007 to ~1.024 million ha per year in 2008–2014. All of this points to the need to assess the effects of clear cutting on atmosphere-ecosystem exchange processes in Russian forests and its consequences for climate system. There are still few experiments describing the temporal patterns of sensible heat,  $CO_2$  and water vapor flux at post-harvest forest ecosystems in Russia (e.g. Machimura et al., 2005; Molchanov et al., 2017) and modeling studies describing possible effects of deforestation and afforestation on regional weather conditions (Kuzmina et al., 2017; Olchev et al., 2018).

The aim of this study was to quantify the consequences of clear cutting on energy,  $CO_2$  and  $H_2O$  exchange between forest ecosystems and the atmosphere using simultaneous meteorological and eddy

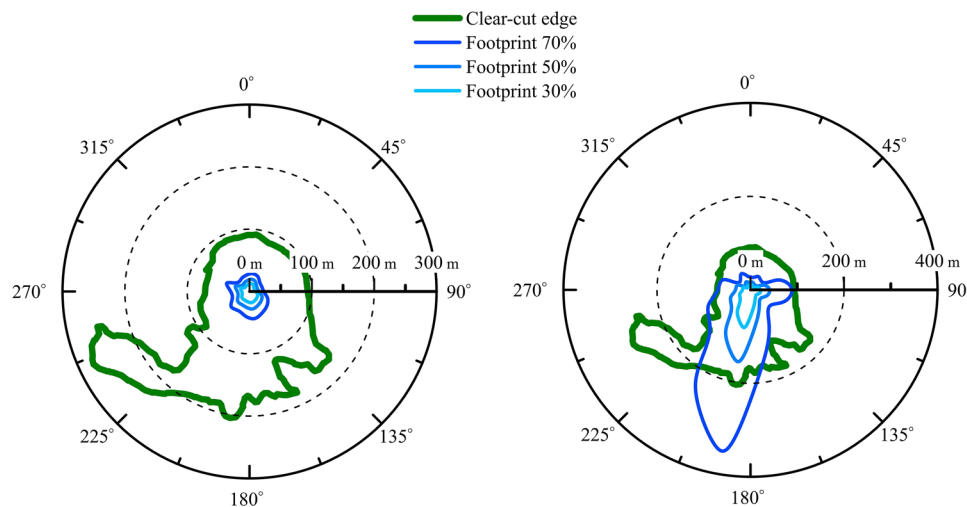


Fig. 2. Daytime (a) and nighttime (b) flux footprint shapes for CC site.

covariance measurements in an undisturbed mature spruce forest and recently clear-cut area within the European southern taiga zone during the first growing season following harvest and to describe the response of atmospheric fluxes to changes in environmental parameters at both sites.

## 2. Materials and methods

### 2.1. Study sites

This study focused on two neighboring (undisturbed mature and harvested) forest ecosystems located in the sustainable management zone of the Central Forest Biosphere Reserve (CFBR) in the south-western part of Valdai Hills in Tver region of Russia, far away from sources of any industrial pollution (Fig. 1). The sites were located ~8 km apart and had very similar weather conditions (Fig. 2).

The study area belongs to the humid continental climate (Dfb type in the Köppen-Geiger classification scheme) (Peel et al., 2007). According to long-term observations at the nearest meteorological station “Zapovednik” (56°30'N, 32°50'E) the mean annual temperature at 2 m height for the period of 1963–2016 was 4.3 °C (−8.5 °C for January and 15.1 °C for July) and average annual precipitation was 720 mm. Snow cover typically persists from mid-November to late March or early April (Desherevskaya et al., 2010; Ivanov et al., 2017). The region is characterized by relatively moist conditions, with annual precipitation exceeding potential evapotranspiration (*PET*; Kuricheva et al., 2017). The Climate Moisture Index (CMI) (Willmott and Feddema, 1992), calculated as the difference between annual precipitation and *PET*, ranged between 0.3–0.4 (Novenko et al., 2018).

The vegetation cover of the CFBR is represented by typical plant communities of southern taiga, which are widespread in the north-eastern part of Europe. The mature spruce forest site (SF) named as Ru-Fyo2 in FLUXNET datasets (56.4617°N, 32.9239°E, 265.00 m a.s.l.) represents a typical undisturbed (with age up to 200 years) nemorose spruce forest of European southern taiga with stem density of Norway spruce (*Picea abies*) - 53%, Norway maple (*Acer platanoides*) - 18%, Scotch elm (*Ulmus glabra*) - 6.4%, Eurasian aspen (*Populus tremula*) - 6% and White birch (*Betula pubescens*) - 5%. The understory is represented mainly by male-fern (*Dryopteris filix-mas*) and wood-sour (*Oxalis acetosella*) (Kurbatova et al., 2008; Kuricheva et al., 2017). Waterlogged micro-sites are covered by various moss species. Tree height reaches 30–35 m. The site lies on a flat plain with well-drained sod-pale podzolic soils. Content of organic carbon in the upper soil horizons varied between 2.67 and 4.67%.

The clear-cut site (CC) (56.444°N, 33.048°E, 250 m a.s.l.) has a

harvested area about 4.5 ha and is also located on a flat area with a gentle slope of about one degree. The forest covering the site before timber harvesting in February–April of 2016 was mainly represented by a Norway spruce (*Picea abies*), White birch (*Betula pubescens*) and Eurasian aspen (*Populus tremula*). Most of the wood was removed from the site when the clear-cut occurred, but a large amount of litter and harvest residue remained on the ground. The clear-cut was free of vegetation until the second half of April 2016. Active regeneration of herbaceous plants started in May (immediately after the ground defrosted). The herbaceous plant community was represented by starwort (*Stellaria graminea*), sow-tit (*Fragaria vesca*) and wood-sour (*Oxalis acetosella*). The active growth of juvenile aspen (*Populus tremula*) trees began that July. After clear-cutting the leaf area index (*LAI*) of vegetation increased from 0 in April to 2.5 m<sup>2</sup> m<sup>−2</sup> in the first week of August. The height of re-grown vegetation reached 70–90 cm during the period while the height of the surrounding forest varied from 18 to 22 m. The CC site is situated on sod-pale podzolic soils with the organic carbon content ranged between 2.73 and 5.79%.

### 2.2. Eddy covariance and meteorological measurements

The flux tower at SF site has a height of 42 m and it is located in the central part of a large uniform forest tract in the southern part of CFBR. The eddy covariance system was mounted on the top of the tower and included enclosed CO<sub>2</sub>/H<sub>2</sub>O gas analyzer LI-7200 A (LI-COR Inc., USA) and 3-D ultrasonic anemometer WindMaster Pro (Gill Instruments, UK).

Meteorological measurements at SF site were performed by automatic humidity and air temperature probe - Vaisala HMP155 (Vaisala Inc., Finland). Precipitation rate was measured using two rain gauges TR-525 M (Texas Electronics Inc., USA) installed at the heights 30 and 2 m. Short-wave incoming and reflected, long-wave incoming and outgoing radiation were measured using 4-component radiometer CNR4 (Kipp & Zonen B.V., The Netherlands) at the height of 41 m. In addition, the incoming photosynthetically active radiation (PAR) was also measured using quantum sensor LI-190R (LI-COR Inc., USA). Soil temperature and volumetric soil water content were measured using three reflectometers Stevens Hydro Probe II (Stevens Water monitoring Systems Inc., USA) at the depth of 10 cm. Soil heat flux measurements were performed by three self-calibrating HFP01SC (Hukseflux Thermal Sensors, The Netherlands) sensors installed at the depth of 5 cm in mineral soil layer around the flux tower. The eddy covariance data were collected using Analyzer interface unit LI-7550 (LI-COR Inc., USA) with frequency of 10 Hz. An acquisition of the additional meteorological data carried out by applying a LI-COR Biomet system 103 (LI-COR Inc., USA) with frequency of 1 min.

The measurement station at CC site was installed immediately after the harvest in the clear-cut area in April 2016. The measurement of soil temperature and soil water content (SWC) was started May 19th because of the frozen ground. The equipment was mounted on a 3 m tripod (CM 106B, Campbell Sci.Inc., USA) which was placed in the central part of the clear-cut in 90 m from the northern edge and about 200 m - from the southern one. This location was chosen with allowing for prevailed southern wind direction in the summer period. Eddy covariance system included CO<sub>2</sub>/H<sub>2</sub>O gas open-path analyzer LI-7500 A (LI-COR Inc., USA) and 3-D ultrasonic anemometer WindMaster Pro (Gill Instruments, UK). The instruments were mounted at the height of 2.4 m above the ground surface. Eddy covariance data was collected on the flash-drive using Analyzer interface unit LI-7550 (LI-COR Inc., USA) at a frequency of 10 Hz.

The system for meteorological observations included an automatic weather transmitter WXT 520 (Vaisala Inc., Finland) for measurements of the air temperature, relative humidity, atmospheric pressure, precipitation rate and duration, wind speed and direction (Mamkin et al., 2016). The WXT 520 was mounted at height of 2 m above the ground. Short-wave incoming and reflected, as well as long-wave incoming and outgoing radiation were measured using 4-component radiometer NR01 (Hukseflux Thermal Sensors, The Netherlands) at the height of 1.9 m. Quantum sensor LI-190R (LI-COR Inc., USA) was used for measurements of incoming PAR. Four reflectometers CS655 (Campbell Sci. Inc., USA) were installed around the tripod in the soil at the 10 cm depth to obtain the temperature and volumetric water content characteristics of the upper soil horizon. Soil heat flux was measured using three heat flux sensors HFP01SC (Hukseflux Thermal Sensors, The Netherlands) at the depth of 5 cm. All meteorological parameters were sampled using data logger CR3000 (Campbell Sci. Inc., USA) at a frequency 0.1 Hz and averaged over 30 - min time intervals. The Eastern European time (UTC + 2) was used for data storage.

### 2.3. Flux calculation, footprint and gap-filling

All steps of data post-processing were performed by the generally accepted recommendations for data analysis (Aubinet et al., 2012; Burba, 2013). The *NEE* of CO<sub>2</sub>, *LE* and *H* fluxes were calculated from the raw data for 30-min time intervals using EddyPro data processing software (LI-COR Inc., USA), which implemented the required statistical tests and corrections. Quality check included 0–2 flag policy (Mauder and Foken, 2006). The CO<sub>2</sub> and heat storage terms in the canopy air space were calculated according to Migliavacca et al. (2009) and Papale et al. (2006). Above ground canopy storage was derived using a process-based model (Oltchev et al., 2002; Falge et al., 2005). After data post-processing all fluxes with flag 2, as well as fluxes with flag 0 and 1, containing the spikes, associated with e.g. rain and dew events, weak turbulence and low wind, were removed from the data sets. The *NEE* data sets were also filtered out based on an analysis of the friction velocity (*u\**) threshold criteria. The threshold values of *u\** calculated for the whole measurement period for the SF and CC sites were 0.380 and 0.086 m s<sup>-1</sup>, respectively.

In filtering low quality data, special attention was paid to footprint analysis. The footprints at both sites were estimated using the model suggested by Kljun et al. (2004). The large uniform forest area around the flux tower at SF site provides very good fetch conditions for flux measurements. The footprint analysis showed that about 70% of daytime and nighttime footprints were located within the uniform forest area around flux tower. The mean 70% fetch length expanded to 259 m in the daytime and to 1011 m at night, respectively. The mean daily 70% fetch length was 623 m. The fetch size for CC site varied significantly depending on time of day and weather conditions. The mean daily 70% fetch length was about 99 m. It was about 31 m in the daytime and it is varied between 27 and 350 m at night depending on the sector of the upwind area. Thus, a large part of 70% fetch lengths at night overstepped the clear-cut border. The fluxes measured during

these periods were excluded from our data analysis.

To assess the possible influence of horizontal advection on turbulent flux measurements at the CC site additional numerical experiments were performed using a two-dimensional turbulent exchange model (Mukhartova et al., 2015; Oltchev et al., 2017). Results of the model simulations showed that the turbulent flux measurements at the mast location and at the height of equipment installation were not significantly influenced by the surrounding forest stand in case of the south and south-west wind directions, under well-developed turbulence and neutral or unstable atmosphere stratification (Mamkin et al., 2016).

There were relatively large gaps in flux time series after excluding non-representative flux data caused mainly by poor weather conditions (e.g. low wind, rain and dew events). Over the study period, flux measurements were missing at the SF site for 19% of *H*, 18% of *LE* and 16% of *NEE* time steps, while at the CC site there were data missing from 18% of *H*, 32% of *LE*, and 43% of *NEE* time steps. The REdDyProc package (Lasslop et al., 2010; Reichstein et al., 2005; Wutzler et al., 2018) was used for filling the gaps in flux data sets and for deriving *NEE* partitioning into *TER* and *GPP*. The mean values of energy balance closure for 30-min intervals were 0.79 for SF site and 0.83 for CC site, respectively. The *H* and *LE* fluxes were also additionally adjusted for closure using the mean daily  $\beta$  following Twine et al (2000) and Aubinet et al. (2012).

### 2.4. Parameterization of *TER* and *GPP* response to change of environmental parameters

To describe the dependence of the key CO<sub>2</sub> budget components such as *GPP* and *TER* on ambient conditions and to find their specific and distinctive features for selected forest ecosystems we used only the flux data that meet the accepted quality criteria. The soil and air temperature were considered as the main factors influencing the *TER* rate. To approximate the dependence between air and soil temperatures and *TER* we used Lloyd - Taylor equation (Lloyd and Taylor, 1994). The best agreement with field data was obtained in case of implementing the combination of the 3-parameter and “restricted” one-parameter forms of the Lloyd - Taylor equations described by Richardson et al. (2006). In the final form the equation for *TER* can be written as:

$$TER = a \exp(-b)/(T + 46.02) \quad (1)$$

where *a* and *b* are empirical parameters, *T* is measured air (*T<sub>a</sub>*) or soil (*T<sub>s</sub>*) temperatures.

Dependence of *TER* on the soil and air temperature we also approximated using *Q<sub>10</sub>* which determines the increase of respiration rate per 10 °C temperature growth (Hashimoto, 2005) and *R<sub>10</sub>* (respiration rate at 10 °C) parameters. According to (Pavelka et al., 2007) *Q<sub>10</sub>* can be expressed by the following equation:

$$Q_{10} = \exp(10\alpha) \quad (2)$$

where  $\alpha$  is parameter taken from the equation describing the temperature - respiration rate dependence in the logarithmic form:

$$\ln(TER) = \alpha T + \gamma \quad (3)$$

where *T* is measured soil (air) temperature and  $\gamma$  is an empirical parameter.

To describe the dependence of *GPP* on incoming *PAR* we used Monsi and Saeki (1953) approximation, which assumes non-linear dependence between *GPP* and *PAR* as:

$$GPP = (a \cdot PAR)/(1 + b \cdot PAR) \quad (4)$$

where *a* and *b* are the coefficients that determine the slope (at *PAR* → 0) and curvature of the non-linear response curve.

To derive the dependence of *GPP* on incoming *PAR* for SF and CC vegetation cover we calculate the photosynthetic light use efficiency ( $\epsilon$ ) that was estimated as a coefficient of the linear equation between *GPP*

and PAR absorbed by ground surface ( $aPAR$ ) (Rosati et al., 2004):

$$GPP = \varepsilon aPAR \quad (5)$$

To calculate  $\varepsilon$  we used daily sums of  $GPP$  and  $PAR$  at both sites. For  $aPAR$  calculation we used incoming and reflected  $PAR$  values. In order to avoid any uncertainties with estimation of  $aPAR$  for very sparse vegetation cover in spring and early summer we selected for our analysis the period from July to September that is characterized by relatively small changes in photosynthesizing biomass at the sites.

Taking into account a high sensitivity of boreal plant communities to temperature changes we also analyzed the possible relationship between  $GPP$  and air temperature for both sites. For data analysis we selected the period characterized by insignificant changes in plant biomass at CC site (July–September) and high incoming  $PAR$  ( $> 800 \mu\text{mol m}^{-2}\text{s}^{-1}$ ). To minimize the influence of high vapor pressure deficit ( $VPD$ ) the data obtained after 14:00 (UTC + 2) were also excluded from our analysis. Thus, to derive the  $GPP$  - temperature relationships we used about 25% of daytime  $GPP$  estimations at the SF site and about 10% - at CC site, respectively.

### 3. Results

#### 3.1. Meteorological conditions

Analysis of meteorological data from SF and CC sites as well from meteorological station “Zapovednik”, situated closely to both selected experimental sites, showed that the study area for the selected measurement period (from April to October 2016) are characterized by relatively warm and moist weather conditions. The mean air temperature for the period was  $2.3^\circ\text{C}$  higher than long-term mean (averaged for period from 1963 to 2013). The daily mean air temperatures (Fig. 3) varied from  $2.6$  to  $22.0^\circ\text{C}$  in spring, from  $8.2$  to  $26.6^\circ\text{C}$  in summer and from  $-0.8$  to  $18.7^\circ\text{C}$  in autumn months. Precipitation was uniformly distributed over the measurement period and totaled  $459\text{ mm}$ , which was about 20% higher than the long-term climatic mean ( $381\text{ mm}$ ). Incoming global solar radiation measured at both experimental sites averaged for the entire measuring period was quite similar: about  $2570\text{ MJ m}^{-2}$  at CC site and  $2910\text{ MJ m}^{-2}$  at SF site.

The albedo of the CC area was characterized by higher absolute values and temporal variability during the measurement period compared with SF site. After timber harvest, the ground surface at CC site was free of any vegetation, and surface albedo varied between 11 and 24%, mainly influenced by a large amount of light-colored litter and harvest residue remained on the ground. Albedo had clear diurnal variability and depended strongly on the wetness of the upper soil layer: albedo of drier surface soil was higher than albedo of wetter soils e.g. after heavy rainfall events. Since the beginning of active vegetation recovery in the second half of June the inter-diurnal albedo variation became less pronounced. Albedo increased slightly to 25% by the end of summer, when  $LAI$  reached maximum values ( $2.5\text{ m}^2\text{ m}^{-2}$ ), mainly due to high reflection properties of herbaceous plant species. The albedo of SF site was characterized by very small seasonal variation and changed around 8% during the entire period under consideration. The mean  $LAI$  of forest canopy at SF site was about  $6.5\text{ m}^2\text{ m}^{-2}$ . Because of different albedo the daily net radiation at both sites differed significantly (Fig. 3): whereas the net radiation of the SF was on average  $9.8 \pm 5.3\text{ MJ m}^{-2}$  per day, the net radiation of CC was much lower - on average  $6.2 \pm 3.2\text{ MJ m}^{-2}$  per day. The net radiation of SF was therefore higher than CC site by about 54%.

The soil temperatures at the 10 cm depth at SF site were always positive for the measurement period from April to late October. The upper soil layer at CC site was completely frozen until the beginning of May. From the middle of May and throughout the measurement period the soil temperature at CC site was always positive. The maximum values of mean daily soil temperatures at SF site were reached at the

end of July (about  $16.0^\circ\text{C}$ ). Mean daily soil temperature at CC site was higher than at SF site from mid-May to September, mainly due to higher global radiation reaching the soil surface. The maximum soil temperature at CC site was observed at the beginning of July ( $20.4^\circ\text{C}$ ). In autumn the soil temperature steadily declined at both sites and was similar in the middle of October at both sites ( $\sim 5.0^\circ\text{C}$ ).

$SWC$  at CC site was slightly higher than at the SF site. The temporal pattern of  $SWC$  at the sites was quite different.  $SWC$  at SF site gradually decreased from  $0.65\text{ m}^3\text{ m}^{-3}$  in April to the  $0.16\text{ m}^3\text{ m}^{-3}$  in September.  $SWC$  at CC site was characterized by lower seasonal variability and decreased during the measurement period from  $0.43\text{ m}^3\text{ m}^{-3}$  in May to  $0.36\text{ m}^3\text{ m}^{-3}$  in September. Thus, with the exception of spring time  $SWC$  at CC site was always slightly higher than at the SF site.

#### 3.2. Turbulence and thermal stratification conditions of the atmospheric surface layer

The various measuring conditions (including the height of flux measurements), different local microclimate, land surface and vegetation properties at both sites resulted in different seasonal and diurnal patterns of turbulence conditions. Our measurements showed higher  $u^*$  values at SF site compared with CC site. The mean  $u^*$  values for the entire measurement period was  $0.408$  and  $0.155\text{ m s}^{-1}$  at SF and CC sites, respectively. At nighttime  $u^*$  was often close to the threshold  $u^*$  values at both sites ( $u^* = 0.086\text{ m s}^{-1}$  at CC and  $u^* = 0.380\text{ m s}^{-1}$  at SF site, respectively). At midday  $u^*$  at SF site reached  $1.7\text{ m s}^{-1}$  while  $u^*$  at CC site usually did not exceed  $0.4\text{ m s}^{-1}$ .

The diurnal variation of atmospheric thermal stratification was more pronounced at CC site where it sharply changed from very stable to very unstable conditions in the morning hours and returned to unstable conditions during the evening. At SF site the atmospheric stratification conditions at the sunrise and sunset times were close to neutral. According to classification suggested by Tzvang et al. (1973) the neutral atmospheric stratification is characterized by the Monin-Obukhov stability parameter ( $1/L$ ) ranged between  $-0.01$  and  $0.01$  and it was observed at SF site in 51% of cases, whereas the stable stratification ( $0.01 < 1/L < 0.1$ ) - in 40% of cases, only. During the daytime the neutral atmospheric stratification at the SF site prevailed in 71% of cases, whereas unstable conditions ( $-0.01 < 1/L < -0.1$ ) were only observed in 22% of cases. The daytime atmospheric conditions at CC site were predominantly characterized by unstable (51%) and very unstable ( $1/L < -0.1$ ) conditions (31%), respectively. About 34% of nighttime measurements at CC site occurred under very stable ( $1/L > 0.1$ ) and 25% under stable conditions ( $0.01 < 1/L < 0.1$ ).

#### 3.3. Seasonal variations of energy balance components

The temporal variability of  $H$  and  $LE$  fluxes were characterized by clear seasonal trends with observed maximum values for  $H$  in May and at the beginning of June for both experimental sites, and with maximums of  $LE$  in June–July for SF and in the second half of July for CC site. In the spring  $H$  changed from  $-1.4$  to  $8.9\text{ MJ m}^{-2}\text{d}^{-1}$  at SF and from  $-0.4$  to  $7.6\text{ MJ m}^{-2}\text{d}^{-1}$  at CC (Fig. 4), whereas  $LE$  varied between  $0.8$  and  $8.9\text{ MJ m}^{-2}\text{d}^{-1}$  in SF and between  $0.0$  and  $6.6$  at CC site. Observed increase of turbulent fluxes from April to May at both sites was mainly influenced by the increase in surface net radiation. Analysis of the Bowen ratio ( $\beta = H/LE$ ) showed a relatively high day-by-day variation of  $\beta$  during this period. The mean  $\beta$  values for both sites in spring were slightly different: they were somewhat larger for SF ( $\beta = 0.9$ ) than for CC site ( $\beta = 0.7$ ). While  $H$  reached maximum values and began to decrease in June, the  $LE$  fluxes at the beginning of summer continued to increase mainly due to large amounts of precipitation providing sufficient soil moisture conditions for both sites. The  $LE$  fluxes reached maximum values at SF site ( $13.2\text{ MJ m}^{-2}\text{d}^{-1}$ ) in the second half of June and at the beginning of July mainly due to high net radiation and air temperature, as well as optimal soil moistening conditions. The  $LE$

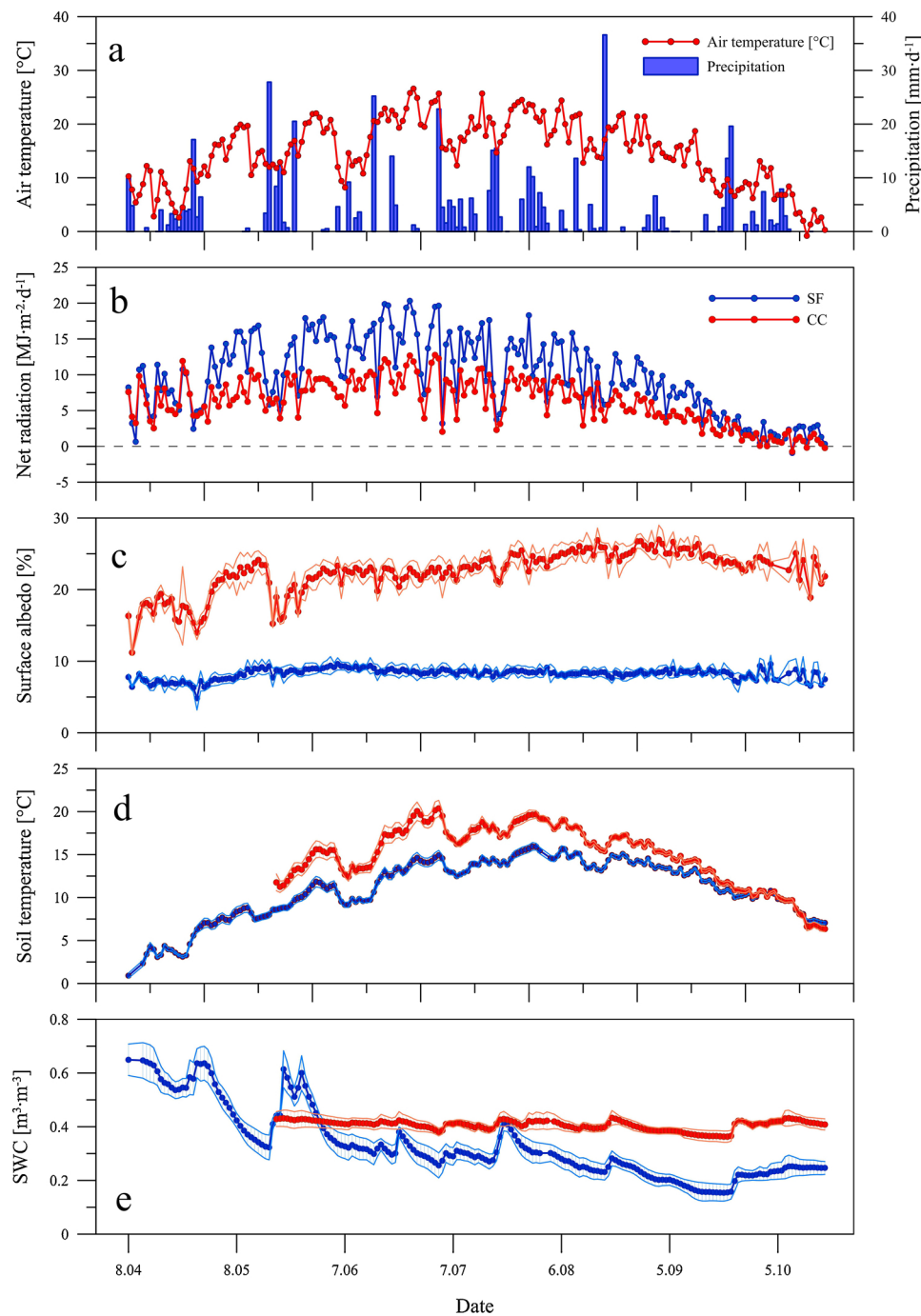


**Fig. 3.** Seasonal courses of mean daily temperature and daily precipitation (a) for year 2016 measured at the “Zapovednik” weather station situated close to both experimental sites, as well as the temporal variability of the net radiation (b), surface albedo (c), soil temperature (d) and (e) soil water content, SWC (e) with standard deviations ( $\pm$  SD) measured at SF and CC sites.

maximum ( $8.9 \text{ MJ m}^{-2} \text{ d}^{-1}$ ) at the CC site shifted to the end of July due to active regeneration of vegetation cover and, especially, fast growing juvenile aspen trees and diverse herbaceous species. While the mean LAI of regenerated vegetation at CC site at the end of June was about  $1 \text{ m}^2 \text{ m}^{-2}$ , one month later it reached  $2.5 \text{ m}^2 \text{ m}^{-2}$ .

The second half of summer was characterized by relatively low day-by-day variation of  $\beta$  as well as  $H$  and  $LE$  fluxes. The mean  $\beta$  values in August were about 0.3 for SF and 0.4 for CC site. In the autumn the  $H$  and  $LE$  fluxes gradually decreased because of declines in net radiation. The  $H$  fluxes during this period varied around 0 from  $-2.5$  to  $1.8 \text{ MJ m}^{-2} \text{ d}^{-1}$  for SF and from  $-0.9$  and  $2.3 \text{ MJ m}^{-2} \text{ d}^{-1}$  for CC sites. The daily  $LE$  fluxes significantly exceed  $H$  and ranged between  $-0.4$  and

$8.1 \text{ MJ m}^{-2} \text{ d}^{-1}$  for SF and between  $0.3$  and  $5.3 \text{ MJ m}^{-2} \text{ d}^{-1}$  for CC site, respectively. The mean  $\beta$  value decreased during the period to 0.17 for SF and to 0.28 for CC sites, respectively (Fig. 4).

The total amount of available energy that ecosystems spent on the  $H$  and  $LE$  fluxes during the entire measuring period was:  $567 \text{ MJ m}^{-2}$  for  $H$  and  $1201 \text{ MJ m}^{-2}$  for  $LE$  at SF site and  $441 \text{ MJ m}^{-2}$  for  $H$  and  $851$  for  $LE$  - at CC site, respectively. Thus, the mean total  $H$  and  $LE$  flux rates for SF site were higher than for CC site by 22 and 48%, respectively (Fig. 5). The evapotranspiration of SF ecosystem for the entire period of measurements reached 601 mm while for CC site it didn't exceed 340 mm.

The temporal variability of soil heat flux ( $G$ ) was less pronounced at

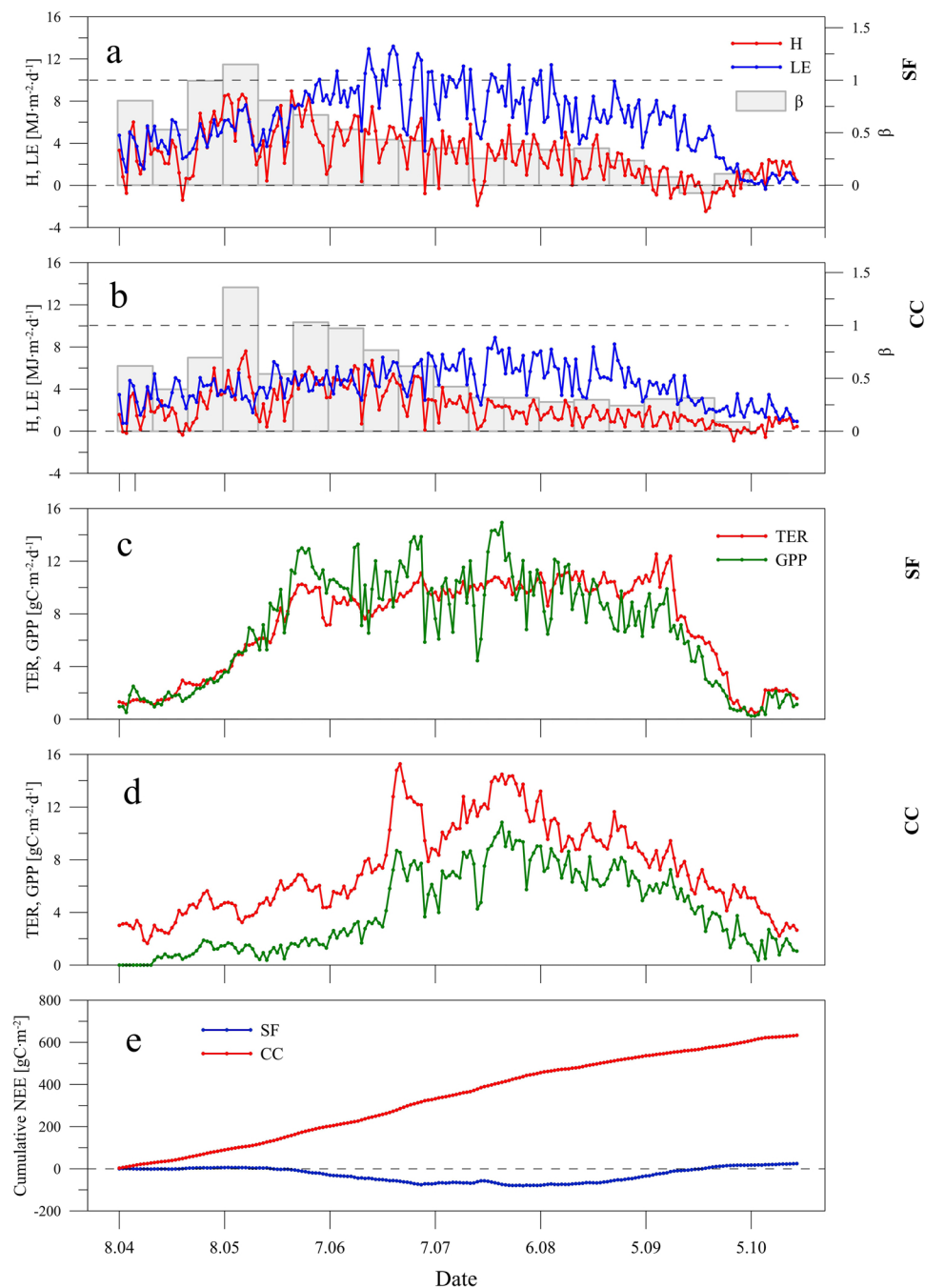


**Fig. 4.** Seasonal courses of the energy and CO<sub>2</sub> fluxes at SF and CC sites (a) daily sensible ( $H$ ) and latent ( $LE$ ) heat fluxes at SF site with Bowen ratio ( $\beta$ ), (b) daily  $H$  and  $LE$  fluxes at CC site with Bowen ratio ( $\beta$ ), (c) daily total ecosystem respiration ( $TER$ ) and gross primary production ( $GPP$ ) at SF site, (d) daily  $TER$  and  $GPP$  at CC site and (e) cumulative  $NEE$  for both sites. Bowen ratios are calculated as a mean for 10-day time intervals.

SF than at CC site, and the mean  $G$  fluxes at SF site were lower than at CC site both for day and night time on average by about 32%.

### 3.4. Seasonal variations of CO<sub>2</sub> fluxes

The seasonal course of  $NEE$  was characterized by large temporal variability that was governed by various abiotic (weather conditions, soil moisture, etc.) and biotic (vegetation regeneration at CC site, phenology) factors. The  $NEE$  at SF site was almost negative during the spring and the first half of summer and then positive in the late summer and in autumn (Fig. 4). The total  $NEE$  averaged for the entire measurement period for SF was close to zero ( $24.3 \text{ gC}\cdot\text{m}^{-2}$ ). The CC site was a consistent source of CO<sub>2</sub> to the atmosphere during the entire

measurement period ( $633.6 \text{ gC}\cdot\text{m}^{-2}$ ). Mean daily  $NEE$  was  $0.1 \pm 1.9 \text{ gC}\cdot\text{m}^{-2}\cdot\text{d}^{-1}$  for SF and  $3.3 \pm 1.3 \text{ gC}\cdot\text{m}^{-2}\cdot\text{d}^{-1}$  for CC site, respectively.

There was no significant difference in  $TER$  between sites: the mean daily  $TER$  was  $7.1 \pm 3.6 \text{ gC}\cdot\text{m}^{-2}\cdot\text{d}^{-1}$  at SF site and  $7.4 \pm 3.4 \text{ gC}\cdot\text{m}^{-2}\cdot\text{d}^{-1}$  at CC site. Differences in  $GPP$  were more pronounced: the mean daily  $GPP$  for the entire measurement period was  $7.0 \pm 4.1 \text{ gC}\cdot\text{m}^{-2}\cdot\text{d}^{-1}$  for SF and  $4.1 \pm 3.0 \text{ gC}\cdot\text{m}^{-2}\cdot\text{d}^{-1}$  for CC sites.

The CO<sub>2</sub> fluxes in spring at SF site demonstrated a sharp growth of  $TER$  from the  $1.0$  to  $10.1 \text{ gC}\cdot\text{m}^{-2}\cdot\text{d}^{-1}$  and  $GPP$  from  $0.5$  to  $13.0 \text{ gC}\cdot\text{m}^{-2}\cdot\text{d}^{-1}$ . Daily  $TER$  and  $GPP$  in summer were  $\sim 10.0 \text{ gC}\cdot\text{m}^{-2}\cdot\text{d}^{-1}$  with standard deviation (SD) about  $0.9 \text{ gC}\cdot\text{m}^{-2}\cdot\text{d}^{-1}$  for  $TER$  and  $2.2 \text{ gC}\cdot\text{m}^{-2}\cdot\text{d}^{-1}$  for  $GPP$ . In the autumn  $TER$  and  $GPP$  sharply decreased to about  $0.5 \text{ gC}\cdot\text{m}^{-2}\cdot\text{d}^{-1}$ .

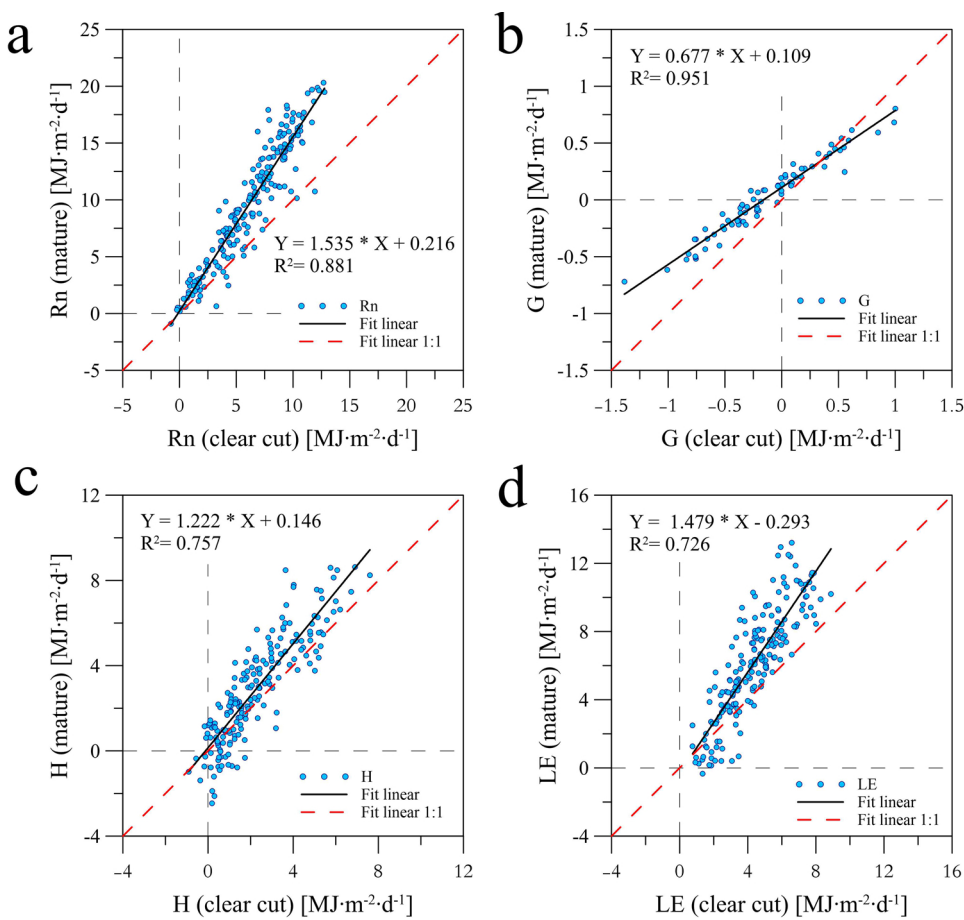


**Fig. 5.** Comparisons of the energy balance components at SF and CC sites: (a) net radiation, (b) ground heat flux ( $G$ ), (c) sensible heat flux ( $H$ ) and (d) latent heat flux ( $LE$ ). Red dotted line correspond to 1:1 line, and black solid line - linear regression describing the dependence of energy balance components at SF from CC sites (For interpretation of the references to colour in this figure legend, the reader is referred to the web version of this article).

The daily  $TER$  at the CC site grew gradually from  $1.6 \text{ gCm}^{-2}\text{d}^{-1}$  to  $15.3 \text{ gCm}^{-2}\text{d}^{-1}$  from April–June and  $GPP$  increased from  $0.0 \text{ gCm}^{-2}\text{d}^{-1}$  in April to  $10.8 \text{ gCm}^{-2}\text{d}^{-1}$  in July. In the second half of summer and in autumn the  $TER$  decreased gradually to the mean values of  $2.2 \text{ gCm}^{-2}\text{d}^{-1}$  (in October). The mean daily  $GPP$  in October was around  $1.0 \text{ gCm}^{-2}\text{d}^{-1}$  with a minimum of  $-0.4 \text{ gCm}^{-2}\text{d}^{-1}$ . Daily  $GPP$  at CC usually exceeded  $GPP$  at SF site by the 60% during October.

### 3.5. Diurnal variations of the energy fluxes

To analyze the diurnal variability of  $H$  and  $LE$  fluxes we chose three months related to different seasons of the year (April, August and October 2016) (Fig. 6). The turbulent fluxes in April were characterized by very high  $H$  fluxes at SF site that significantly exceeded  $H$  values at CC site, and by quite similar  $LE$  fluxes for both sites. The relationship of  $H$  and  $LE$  at both sites was significantly differed. Whereas the midday  $H$  fluxes at the SF site were  $202 \pm 67 \text{ Wm}^{-2}$  and approximately twice as high as that  $LE$  ( $103 \pm 38 \text{ Wm}^{-2}$ ), the  $LE$  at the CC site was ( $109 \pm 65 \text{ Wm}^{-2}$ ) just a little higher than  $H$  ( $88 \pm 56 \text{ Wm}^{-2}$ ). Nocturnal fluxes of  $H$  and  $LE$  at SF site were  $-65 \pm 19 \text{ Wm}^{-2}$  and  $-17 \pm 8 \text{ Wm}^{-2}$ , respectively. Nocturnal  $H$  and  $LE$  fluxes at CC site (under well-developed turbulence and southern wind direction) were on average somewhat higher  $-13 \pm 13 \text{ Wm}^{-2}$  and  $3 \pm 5 \text{ Wm}^{-2}$ , respectively. The mean energy balance closure in April was about 0.7 at SF site and 0.72 - at CC site, respectively.

The midday values of  $LE$  ( $242 \pm 67 \text{ Wm}^{-2}$  at SF and  $192 \pm 66 \text{ Wm}^{-2}$  at CC site) in August were consistently higher than the  $H$  fluxes ( $181 \pm 65 \text{ Wm}^{-2}$  at SF site and  $84 \pm 32 \text{ Wm}^{-2}$  at CC site) at both sites. Sum of  $LE$  and  $H$  fluxes ( $LE+H$ ) at SF site exceeded the corresponding sum at CC site by about 50%. The  $G$  flux at the CC site was somewhat higher than at the SF mainly due to higher soil surface

insolation. Daily maximums of  $G$  reached  $22 \pm 8 \text{ Wm}^{-2}$  at CC site, whereas at SF site it was only  $9 \pm 4 \text{ Wm}^{-2}$ . The mean energy balance closure was somewhat larger in August than in April: 0.81 at SF site and 0.80 at CC site, respectively.

The atmospheric fluxes in October were somewhat lower than in spring, but they were characterized by similar ratios between the  $H$  and  $LE$  fluxes as were observed in April. The  $H$  fluxes reached  $113 \pm 66 \text{ Wm}^{-2}$  at SF site and  $56 \pm 47$  at CC site. The  $LE$  fluxes were somewhat lower, averaging  $41 \pm 29 \text{ Wm}^{-2}$  at SF and  $61 \pm 42 \text{ Wm}^{-2}$  at CC site. The mean energy balance closure in October was 0.82 at SF site and 0.8 at CC site, respectively.

### 3.6. Diurnal variations of $\text{CO}_2$ fluxes

The diurnal variation of  $\text{CO}_2$  fluxes was strongly influenced by incoming solar radiation, air and soil temperatures, and vegetation structure (especially at CC site; Fig. 7). The CC site was free of any vegetation in April, during which time variation in  $NEE$  were influenced by  $TER$  dynamics. The  $NEE$  was positive ( $2.3 \pm 1.0 \mu\text{mol}\cdot\text{m}^{-2}\cdot\text{s}^{-1}$ ; carbon source) during the whole day unlike the fluxes at SF site where daytime  $NEE$  was mostly negative ( $-2.2 \pm 1.6 \mu\text{mol}\cdot\text{m}^{-2}\cdot\text{s}^{-1}$ ; carbon sink). Nocturnal  $NEE$  at CC site was positive ( $2.0 \pm 1.0 \mu\text{mol}\cdot\text{m}^{-2}\cdot\text{s}^{-1}$ ) and comparable with the fluxes at SF site.

During summer, both ecosystems became a daytime sink of  $\text{CO}_2$ . Daytime  $NEE$  reached  $-9.9 \pm 5.1 \mu\text{mol}\cdot\text{m}^{-2}\cdot\text{s}^{-1}$  and  $-5.9 \pm 3.0 \mu\text{mol}\cdot\text{m}^{-2}\cdot\text{s}^{-1}$  at SF and CC sites, respectively. Nighttime  $NEE$  was around  $8.8 \mu\text{mol}\cdot\text{m}^{-2}\cdot\text{s}^{-1}$  at both sites. Higher soil temperature amplitude at the CC site provided a larger diurnal variation of  $TER$  than at SF site. The daily maximum  $TER$  was about  $12.1 \pm 1.7 \mu\text{mol}\cdot\text{m}^{-2}\cdot\text{s}^{-1}$  at CC site and about  $11.7 \pm 1.3 \mu\text{mol}\cdot\text{m}^{-2}\cdot\text{s}^{-1}$  in SF ecosystem.

In October, the CC site was an active sink of  $\text{CO}_2$  during the day

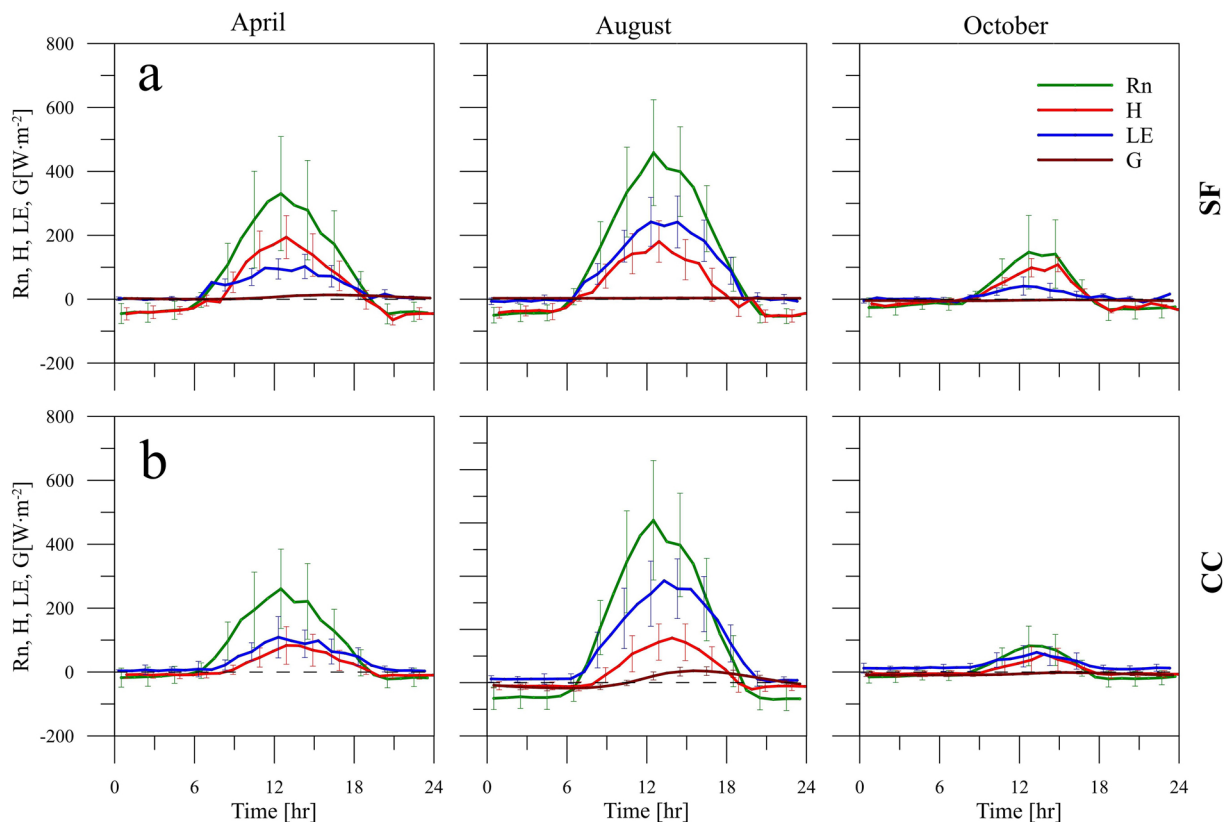


Fig. 6. Diurnal courses of the mean energy balance components for three months (April, August and October) at SF (a) and CC sites (b). Vertical whiskers indicate standard deviations (SD).

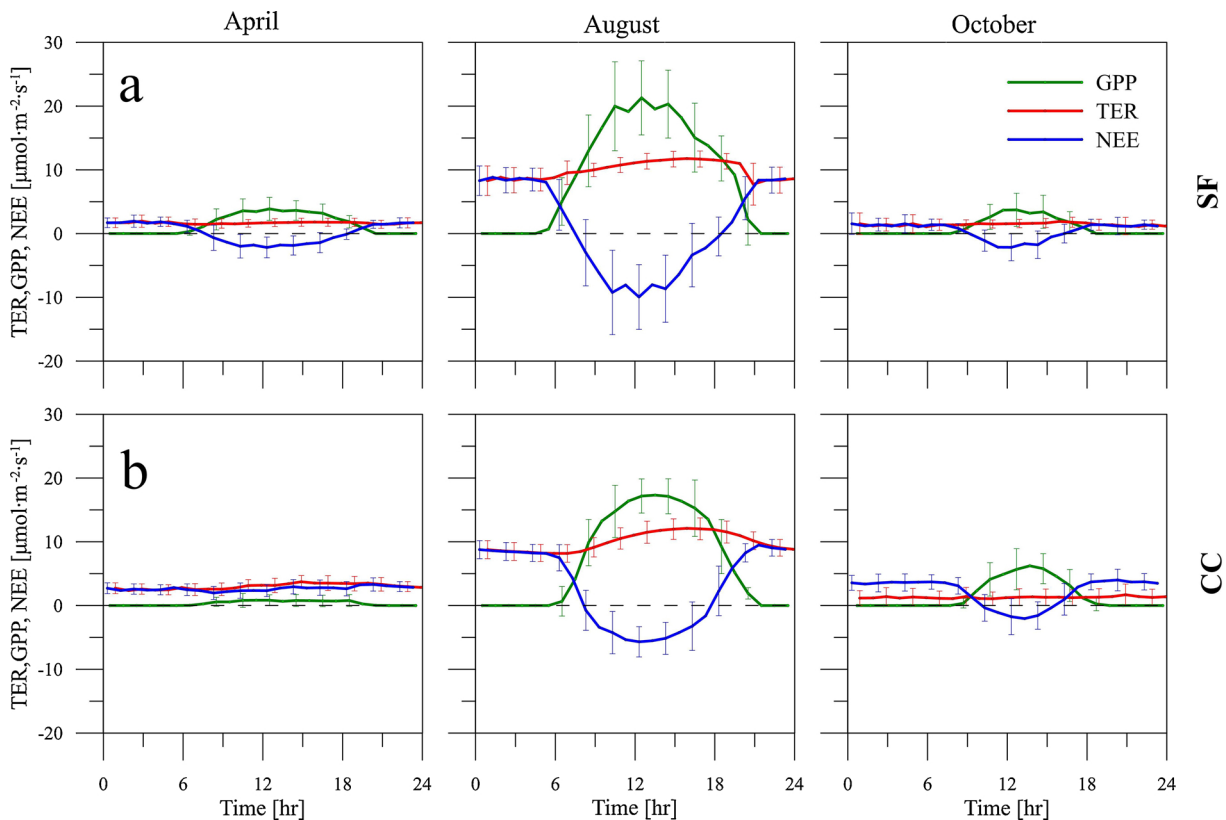
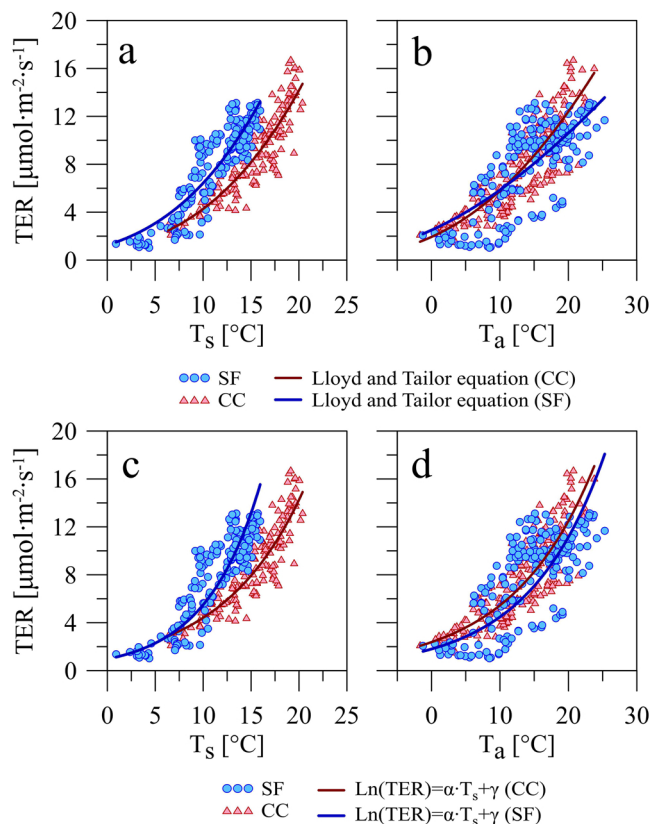


Fig. 7. Diurnal courses of the mean CO<sub>2</sub> balance components for three months (April, August and October) at SF (a) and CC sites (b). Vertical whiskers indicate standard deviations (SD). Negative *NEE* denotes carbon uptake by the ecosystem.



**Fig. 8.** Approximation of the daily *TER* rates from the soil (a, c) and air (b, d) temperature at SF and CC sites by Lloyd and Tailor equation (a, b) and  $Q_{10}$  approach (c, d).

despite a relatively large decrease in *LAI* ( $LAI \sim 1.5 \text{ m}^2 \text{ m}^{-2}$ ). The daily absolute maximums of *NEE* were quite similar at both sites ( $-2.3 \pm 2.4 \mu\text{mol}\cdot\text{m}^{-2}\cdot\text{s}^{-1}$  at SF and  $-2.1 \pm 2.4 \mu\text{mol}\cdot\text{m}^{-2}\cdot\text{s}^{-1}$  at CC site); however, *GPP* was even higher at CC site than at SF site (up to  $3.9 \pm 2.9 \mu\text{mol}\cdot\text{m}^{-2}\cdot\text{s}^{-1}$  at SF site and  $6.3 \pm 2.7 \mu\text{mol}\cdot\text{m}^{-2}\cdot\text{s}^{-1}$  at CC site). The larger *TER* rates at CC site were also indicated. The mean diurnal *TER* rate was  $1.4 \pm 0.9 \mu\text{mol}\cdot\text{m}^{-2}\cdot\text{s}^{-1}$  at SF and  $3.8 \pm 1.9 \mu\text{mol}\cdot\text{m}^{-2}\cdot\text{s}^{-1}$  at CC site, respectively.

**3.7. Dependence of *TER* and *GPP* rates on environmental conditions**

The higher mean daily soil and lower daily air temperatures at the CC compared with SF site resulted in quite different sensitivity of *TER* to changes in temperature (Fig. 8). Soil and air temperature explained about 50% of temporal variability in *TER* at SF site, whereas *TER* was more strongly dependent on soil temperature at CC site (Table 1). Air and soil temperatures at CC explained 72 and 83% of the variability in

**Table 1**

Approximated forms of Lloyd - Tailor equation for *TER* of SF and CC sites as a function of the air and soil temperatures, as well as equations for *GPP* based on *LUE* approach.  $TER_{SF}$ ,  $GPP_{SF}$ ,  $TER_{CC}$  and  $GPP_{CC}$  are *TER* and *GPP* at SF and CC sites, respectively.

Equation	R <sup>2</sup> (p < 0.05)
Clear-cut	
$TER_{CC} = 8275.4 \cdot \exp((-426.5)/(T_s + 46.02))$	0.83
$TER_{CC} = 719.6 \cdot \exp((-271.9)/(T_a + 46.02))$	0.72
$GPP_{CC} = 0.419 \cdot aPAR$	0.93
Undisturbed spruce forest	
$TER_{SF} = 9407.8 \cdot \exp((-414.4)/(T_s + 46.02))$	0.53
$TER_{SF} = 273.9 \cdot \exp((-219.7)/(T_a + 46.02))$	0.50
$GPP_{SF} = 0.270 \cdot aPAR$	0.94

*TER*, respectively.

Calculated  $Q_{10}$  and  $R_{10}$  values for both sites are shown in table (Table 3). The  $R_{10}$  values for SF and CC sites were quite similar for *TER* calculations based on both soil and air temperatures. On the other hand, the  $Q_{10}$  values differed significantly between sites. The  $Q_{10}$  values for SF site were higher than  $Q_{10}$  for CC site. Moreover, the  $Q_{10}$  values calculated using  $T_s$  were larger than  $Q_{10}$  derived from  $T_a$  for both sites. So, provided analysis of temperature response of *TER* using the Lloyd - Tailor equation showed that *TER* rates at both sites are characterized by a higher sensitivity to soil temperature than to air temperature and this relationship is more clearly pronounced for SF compared with CC site (Fig. 8).

To analyze the dependence of *GPP* on *PAR* we selected three contrasting months related to different seasons of the year (April, August and October). In April at CC site under relatively high *PAR* the *GPP* was quite independent of *PAR* mainly due to very sparse green vegetation available in the clear-cut area after timber harvest (Fig. 9). On the contrary, the *GPP* of spruce forest at SF site showed a clear response of *GPP* to *PAR* ( $a = 0.022$ ,  $b = 0.005$ ,  $r^2 = 0.82$ ,  $p < 0.05$ ,  $SD$  of *GPP* is  $1.4 \mu\text{mol}\cdot\text{m}^{-2}\cdot\text{s}^{-1}$ ) (Table 2). The light response curves of *GPP* at both sites in August were quite similar mainly due to active regeneration of herbaceous vegetation and juvenile trees at CC site. The light response curves of *GPP* at SF sites was characterized by slightly lower slope and curvature (SF:  $a = 0.09$ ,  $b = 0.004$ ,  $r^2 = 0.57$ ,  $SD = 5.1 \mu\text{mol}\cdot\text{m}^{-2}\cdot\text{s}^{-1}$ ; CC:  $a = 0.168$ ,  $b = 0.08$ ,  $r^2 = 0.97$ ,  $p < 0.05$ ,  $SD = 3.1 \mu\text{mol}\cdot\text{m}^{-2}\cdot\text{s}^{-1}$ ). *GPP* in October at CC site was somewhat higher than *GPP* of forest vegetation at SF site. The parameters characterizing the light response curve of vegetation at CC site are:  $a = 0.207$ ,  $b = 0.029$ ,  $r^2 = 0.83$  under  $p < 0.05$ . The corresponding parameters of the model for SF site are:  $a = 0.019$ ,  $b = 0.001$ ,  $r^2 = 0.94$  at  $p < 0.05$  and  $SD = 2.1 \mu\text{mol}\cdot\text{m}^{-2}\cdot\text{s}^{-1}$ .

An analysis of the dependence of daily *GPP* on absorbed *PAR* (*aPAR*) for period from July to September 2016 showed a quasi-linear relationship between *GPP* and *aPAR* for both experimental sites (Fig. 10). Application of the simplest model parameterization assuming a linear relationship between daily values of *GPP* and *PAR* allowed us to estimate the light use efficiency ( $\epsilon$ ) for *GPP* that is calculated as the ratio of daily mean *GPP* to daily sums of *aPAR* and characterizes the efficiency with which this absorbed *PAR* is converted by plants to fixed carbon (Monteith, 1977).

Calculations of  $\epsilon$  for *GPP* for both sites showed that the plant canopy at the CC site was characterized by larger  $\epsilon$  than SF site under the present magnitude of *PAR* variability (Table 3) and (Fig. 10). Whereas  $\epsilon$  values for SF site was  $0.27 \text{ gC}\cdot\text{MJ}^{-1}$ ,  $\epsilon$  values of herbaceous vegetation for CC site was about 1.5 times higher ( $\epsilon = 0.42 \text{ gC}\cdot\text{MJ}^{-1}$ ).

Analysis of possible relationships between *GPP* and air temperature showed that within the temperature interval from 0 to 20 °C the *GPP* patterns for both sites were characterized by similar gradual increase of *GPP* with increasing temperature (Fig. 11). For air temperatures higher than 20 °C the *GPP* response to temperature for both sites was quite different. Whereas *GPP* at SF site continued to gradually increase under higher temperatures, *GPP* of vegetation cover at CC site reached maximum values at 23–25 °C and had no substantial changes under higher air temperatures. Taking into account the sufficient soil moisture conditions for the entire study period such trend can be explained by specific response of forest and grassy vegetation to temperature oscillations.

**4. Discussion**

**4.1. Energy fluxes**

Comparisons of the *H* and *LE* fluxes in undisturbed SF and at CC area for the selected period revealed two main relationships: (i) *H* and *LE* fluxes at SF generally exceeded the fluxes at CC site; and (ii) despite a large difference between turbulent fluxes at both experimental sites the temporal patterns of the Bowen ratio at CC and SF sites were very

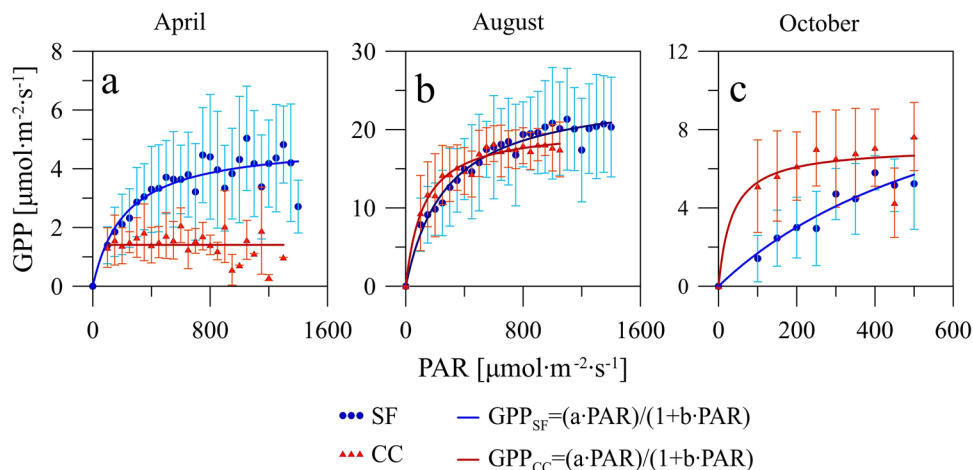


**Fig. 9.** Light response curves of *GPP* for April (a), August (b) and October (c) at SF and CC sites, respectively. The points correspond to the mean *GPP* values for appropriate *PAR* interval ( $50 \mu\text{mol m}^{-2}\text{s}^{-1}$ ). Error bars depict one standard deviation (SD) of *GPP* for each selected *PAR* interval.

**Table 2**

Approximated forms of the light response curve (Eq. 4) for selected months at SF and CC sites.

Month	Equation	R <sup>2</sup> (p < 0.05)
Clear-cut		
August	$GPP_{CC} = (0.168 \cdot PAR) / (1 + 0.008 \cdot PAR)$	0.97
October	$GPP_{CC} = (0.207 \cdot PAR) / (1 + 0.029 \cdot PAR)$	0.83
Undisturbed spruce forest		
April	$GPP_{SF} = (0.022 \cdot PAR) / (1 + 0.005 \cdot PAR)$	0.82
August	$GPP_{SF} = (0.090 \cdot PAR) / (1 + 0.004 \cdot PAR)$	0.97
October	$GPP_{SF} = (0.019 \cdot PAR) / (1 + 0.001 \cdot PAR)$	0.94

**Table 3**

Key parameters describing the energy and CO<sub>2</sub> fluxes at SF and CC sites for the entire measuring period (08.04–18.10 2016).

Parameter	SF site	CC site
<i>H</i> [ $\text{MJ}\cdot\text{m}^{-2}$ ]	567	441
<i>LE</i> [ $\text{MJ}\cdot\text{m}^{-2}$ ]	1201	851
Bowen ratio ( <i>H/LE</i> )	0.47	0.52
<i>ET</i> [mm]	601	340
<i>NEE</i> [ $\text{gC}\cdot\text{m}^{-2}$ ]	24	633
<i>TER</i> [ $\text{gC}\cdot\text{m}^{-2}$ ]	1373	1428
<i>GPP</i> [ $\text{gC}\cdot\text{m}^{-2}$ ]	1349	794
<i>Q</i> <sub>10</sub> (based on <i>T</i> <sub>a</sub> )	2.49	2.29
<i>Q</i> <sub>10</sub> (based on <i>T</i> <sub>s</sub> )	5.73	3.23
<i>R</i> <sub>10</sub> ( <i>T</i> <sub>a</sub> ) [ $\mu\text{mol}\cdot\text{m}^{-2}\cdot\text{s}^{-1}$ ]	5.43	5.61
<i>R</i> <sub>10</sub> ( <i>T</i> <sub>s</sub> ) [ $\mu\text{mol}\cdot\text{m}^{-2}\cdot\text{s}^{-1}$ ]	5.77	4.09
$\epsilon$ [ $\text{gC}\cdot\text{MJ}^{-1}\text{ PAR}$ ]	0.27	0.42

similar (Fig. 4).

The first relationship agrees well with results of numerous studies that reported reductions in net radiation, *H*, and *LE* fluxes in areas during early succession after clear cutting (Amiro, 2001; Amiro et al., 2006; McCaughey, 1985; Rannik et al., 2002). The relatively small change of Bowen ratios after forest clearing could be related to local environmental conditions that may vary from year to year (Amiro et al., 2006). Moreover, they argued that post-disturbance ecosystem recovery in combination with sufficient moistening conditions may be a very important factor controlling changes in evaporation. Local weather conditions and low rates of vegetation regeneration after timber harvest can increase daily *H* and decrease *LE* fluxes. Such dynamics were particularly observed by Rannik et al (2002) in Scots pine forest in Finland, who found from analysis of eddy-covariance data that forest clearing increased the Bowen ratios from 0.26 to 0.47. Actually such changes of Bowen ratios are very small and they are within a range of natural

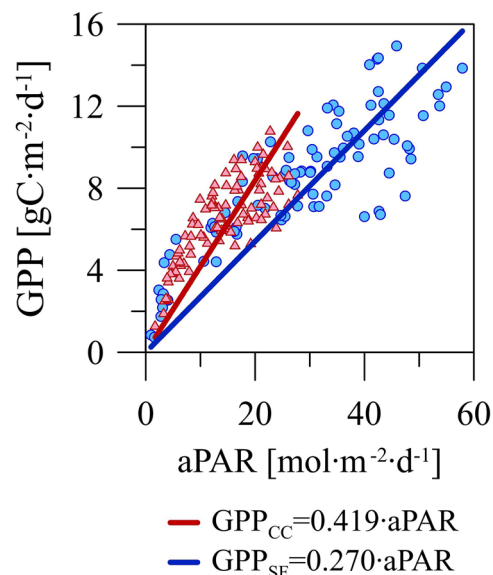


**Fig. 10.** Linear *LUE* curves for daily mean *GPP* and daily sums of *aPAR* for period from July to September.

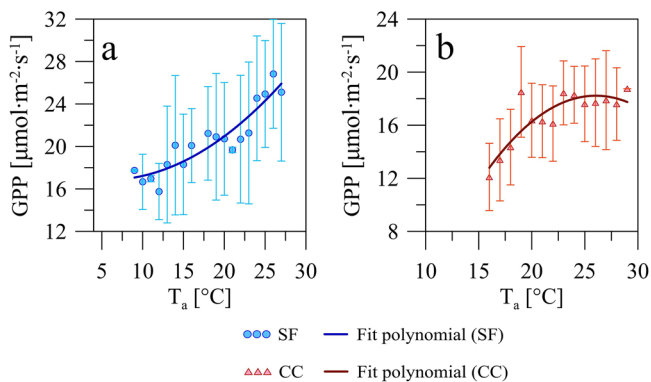


**Fig. 11.** Polynomial curves describing the dependence of *GPP* on air temperature at SF (a) and CC (b) sites. The points correspond to the mean *GPP* values for appropriate *T*<sub>a</sub> interval (1 °C). Error bars demonstrate standard deviation (SD) of *GPP* for each *T*<sub>a</sub> class.

variability of Bowen ratios for e.g. coniferous and deciduous forests in summer aggregated by Wilson et al. (2002) from analysis of Fluxnet data sets.

The reason for very small differences in Bowen ratios between SF and CC site that was observed in our study during the first year following harvest could be warm and very wet weather conditions in the study region that initiated active vegetation recovery within the clear-cut area. Our measurements showed a strong increase of LAI from April to late July at CC site (from 0 to  $2.5 \text{ m}^2 \text{ m}^{-2}$ ) mainly due to a large amount of precipitation providing sufficient soil moisture conditions for plant growth. Similar intensive recovery rate after clear cutting was reported by Humphreys et al. (2006) and Paul-Limoges et al. (2015) in Douglas fir forest in British Columbia. They particularly found that during two years after clearing LAI increased from 0.5 to  $2.2 \text{ m}^2 \text{ m}^{-2}$ . On another hand, some studies indicate a very low rate of vegetation regeneration. For example, Zha et al. (2009) reported that LAI of two-year old clear-cut in Jack pine in Saskatchewan didn't exceed  $0.18 \text{ m}^2 \text{ m}^{-2}$ . Under these conditions the clear-cut evapotranspiration during the first months after timber harvesting is mainly determined by direct soil surface evaporation governed by wetness of the upper soil horizon. In the next year such effects can be lower. In particular Matthews et al. (2017) argued that the interannual variations of the Bowen ratio after wind throw can be very low and that partitioning of turbulent energy mostly depended on evaporative atmospheric demand rather than on post-disturbance ecosystem recovery.

Observed higher values of daily  $H$  and  $LE$  at SF compared with CC site in our study can be explained mainly by higher daily net radiation governed by lower albedo of SF site. Albedo increases at forest clearings were previously also described in numerous experimental studies. Particularly McCaughey (1985) reported about effect of forest clearings on albedo for the mixed forests in Canada and Cherubini et al. (2012) for boreal forest areas in North America and North Europe. According to Cherubini et al. (2012) the timber harvest in a spruce forest in Norway can lead to albedo increase by 29%. The increasing of albedo following stand-replacing disturbances (harvesting, fires, windthrows etc.) is supposed to be usual for dark coniferous and mixed dark coniferous-broadleaf forest ecosystems, due to the replacement of the dark coniferous species by lighter herbaceous and small-leaved tree species after the disturbance (Lyons et al., 2008). A relatively high albedo of bare ground at CC site in spring was mainly driven by a large amount of light-colored litter and harvest residue remained on the ground. Albedo characterized by a clear diurnal variability and depended on the wetness of the upper soil layer. Similar results showing the decrease of surface albedo in rainy periods at the clear-cut site in the mixed coniferous-deciduous forest in Ontario (Canada) were also reported by McCaughey (1987).

Lower  $H$  and  $LE$  at CC site compared with SF in daily course was influenced by surface albedo and attended by differences in soil heat fluxes. The soil heat fluxes measured at CC site were larger than the fluxes obtained at SF site (Fig. 6). Such effects can be mainly governed by different solar radiation and soil temperature conditions of ground surface that were reported in experimental studies provided in different types of boreal and temperate forests with various temperature and moisture conditions (e.g. Amiro, 2001; Amiro et al., 2006).

The various patterns of SWC at CC and SF sites were mainly driven by two factors: different relationships between precipitation and surface evapotranspiration and various ground water levels at both sites. CC site is characterized by permanently high ground water level. During the summer month it never fell lower than 20 cm depth. The precipitation at the site significantly exceeded the surface evapotranspiration by about 28%. The ground water level at SF site was much deeper than at CC site and varied depending on weather conditions between 1.5 and 0.6 m. There were also several episodes of sharp increasing the water level after heavy rainfalls: ground water level grew at SF site for short time periods to the level of 10–20 cm. The summer evapotranspiration at SF site was some higher than precipitation amount

by about 7%.

#### 4.2. Carbon dioxide fluxes

Comparisons of the temporal variability of  $NEE$ ,  $GPP$  and  $TER$  at SF and CC sites showed that the  $\text{CO}_2$  balance components differed significantly between sites in contrast to energy fluxes which were characterized by similar seasonal patterns. Whereas the daily  $NEE$  at CC site were always positive ( $\text{CO}_2$  source) during the entire period of flux measurements, the  $NEE$  of undisturbed SF site for the period changed from negative ( $\text{CO}_2$  sink) in spring and early summer to positive ( $\text{CO}_2$  source) in late summer and autumn (Fig. 4).

Removing the large amount of photosynthesizing biomass from CC site can obviously result in a significant reduction of  $GPP$  compared with the undisturbed SF site, which in turn can lead to change of  $NEE$ . Amiro et al. (2010) aggregated the results of flux measurements at several disturbed forest ecosystems in North America and showed that harvesting slightly decreases  $TER$  rates of forest ecosystems, whereas the main changes to the  $\text{CO}_2$  balance were caused by decreased  $GPP$ . According to these estimates the decrease of  $TER$  after timber harvesting can range between 15 and 60%. Kolari et al. (2004) analyzed the temporal pattern of  $TER$  at a 4-year old clear-cut in Finland and found that the  $TER$  rates at the clear-cut site were similar to those of undisturbed mature Scots pine forest. Our analysis showed that  $TER$  was similar at SF and CC sites, suggesting that clear cutting in this area does not significant affect  $TER$  (Fig. 4). These results are confirmed by  $TER$  measurements conducted at CC site in summer 2016 using the chamber methods (Mamkin et al., 2016). The  $TER$  rates estimated by chamber method varied between 4.4 and  $10.9 \text{ gC}\cdot\text{m}^{-2}\cdot\text{d}^{-1}$  and they showed good agreement with eddy covariance data. The possible reasons for very high  $TER$  rates at our CC site can be a very high emission of  $\text{CO}_2$  from soil surface caused by decay of fine and coarse roots of harvested trees and a large amount of litter and residue remaining at CC after timber harvesting under relatively warm and wet weather conditions (Garrett et al., 2012; Molchanov et al., 2017).

The decrease in mean  $GPP$  for the growing season after timber harvesting was also less pronounced in our study. For instance, the decrease in  $GPP$  was only about 70% of the mean  $GPP$  reduction rates reported in other experiments. For example, Kowalski et al. (2003) found a three-fold decrease of  $GPP$  in a recently clear-cut site in a Fern and Pine forest in Southwest France. Paul-Limoges et al. (2015) reported about 14.5-fold reduction of  $GPP$  after timber harvesting at 1-year clear-cut in Douglas Fir forest in British Columbia. High  $GPP$  rate at CC site in our case was mainly influenced by active vegetation regeneration in the summer supported by relatively high air temperature and large amount of precipitation uniformly distributed over the entire period of measurements that provided sufficient soil water content close to the soil field capacity.

Comparisons of our  $\text{CO}_2$  flux measurements at CC site with available experimental data obtained by different research teams at clear-cuts of different ages in different forest types under various thermal and moistening conditions showed a high diversity of  $NEE$ ,  $GPP$  and  $TER$  patterns (Table 4). The CC site was characterized by relatively high  $TER$  in comparison with other experimental sites. Moreover, the  $TER$  rates were significantly higher than  $GPP$ , which resulted in a large net  $\text{CO}_2$  flux into the atmosphere (Fig. 12). A similar relatively high  $NEE$  was obtained by Williams et al. (2014) for 1-year clear-cut in spruce forest in Massachusetts. Due to enhanced  $TER$  and  $GPP$  values the  $\text{CO}_2$  balance of the area was very close to our CC site (Fig. 12). Moreover our  $NEE$  estimates at CC site are also comparable with  $\text{CO}_2$  fluxes obtained by e.g. Paul-Limoges et al. (2015) for fresh clear-cut in Douglas fir forest in British Columbia ( $NEE = 4.1 \text{ gC}\cdot\text{m}^{-2}\cdot\text{d}^{-1}$ ), with  $NEE$  estimates at 3–4 year clear-cut in Red spruce forest in Alaska (Gordon et al., 1987; Pypker and Fredeen, 2002) ( $NEE = 3.4 \text{ gC}\cdot\text{m}^{-2}\cdot\text{d}^{-1}$ ) and with  $NEE$  at 5-year Scots pine clear-cut in southern Finland (Rannik et al., 2002) ( $NEE = 4.0 \text{ gC}\cdot\text{m}^{-2}\cdot\text{d}^{-1}$  for July and August and  $2.5 \text{ gC}\cdot\text{m}^{-2}\cdot\text{d}^{-1}$  for

**Table 4**  
Literature syntheses of CO<sub>2</sub> flux measurements from clear-cut areas in boreal and sub-boreal forest ecosystems.

Reference	Location	Dominant tree species	Method	Clear-cut age [yrs]	Period	NEE [gCm <sup>-2</sup> d <sup>-1</sup> ]	TER [gCm <sup>-2</sup> d <sup>-1</sup> ]	GPP [gCm <sup>-2</sup> d <sup>-1</sup> ]
<b>Present study</b>	<b>Vaidai Hills (Western Russia)</b>	<b>Norway spruce, Norway maple, Scotch elm, Eurasian aspen, White birch</b>	<b>Eddy covariance</b>	<b>0</b>	<b>Apr-Oct</b>	<b>3.3</b>	<b>7.4</b>	<b>4.1</b>
Aguilos et al., 2014	Hokkaido (Japan)	Mongolian Oak, Erman's Birch, Japanese white birch Sakhalin fir (planted by 2-year old hybrid larch seedlings)	Eddy covariance	0	year	1.6	2.9	1.3
				1	year	1.4	2.8	1.5
				2	year	0.4	3.2	2.8
				3	year	0.3	3.1	2.8
				4	year	0.0	3.4	3.4
				5	year	0.3	3.3	3.1
				6	year	0.1	2.9	2.8
				7	year	-0.1	3.3	3.4
				8	year	-0.1	3.1	3.2
Amiro, 2001	Alberta (Canada)	Trembling aspen, Balsam poplar	Eddy covariance	1	July	1.6	-	-
Amiro et al., 2006	Saskatchewan (Canada)	Jack Pine	Eddy covariance	7	year	0.2	-	-
				8	year	0.2	-	-
Fernandez et al., 1993; Pypker and Fredeen, 2002	Maine (USA)	Red Pine	Alkali absorption technique	4	May-Sep	2.1	-	-
Giasson et al., 2006	Quebec (Canada)	Black spruce	Eddy covariance	2	year	0.3	1.2	0.9
Gordon et al., 1987; Pypker and Fredeen, 2002	Alaska (USA)	Red Spruce	Soda lime technique	3-4	May-sep	3.4	-	-
Humphreys et al., 2006	British Columbia (Canada)	Douglas Fir	Eddy covariance	2	year	1.7	2.9	1.2
Kolari et al., 2004	Finland	Scots Pine	Eddy covariance	4	Jul-Oct	1.4	3.2	1.8
Kowalski et al., 2003	Les Landes (Southeastern France)	Maritime pine	Eddy covariance	1	year	0.8	2.7	0.8
Lytle, Cronan, 1998; Pypker and Fredeen, 2002	Maine (USA)	Red spruce, Balsam fir, White pine, Red maple, Paper birch	Soda lime technique	0	May-Nov	2.4	-	-
Machimura et al., 2005	Yakutia (Russia)	Dahurian larch	Eddy covariance	0	May-Sep	1.7	-	-
				1	May-Sep	1.6	-	-
				2	May-Sep	0.6	-	-
Paul-Limoges et al., 2015	Vancouver island (British Columbia, Canada)	Douglas Fir (planted with 1-year Douglas Fir and Sitka spruce seedlings)	Eddy covariance	0	May-Oct	4.1	4.5	0.4
				1	May-Oct	2.4	4.2	1.7
Pypker and Fredeen, 2002	British Columbia (Canada)	Spruce-Fir (planted by 2-year hybrid white spruce and lodgepole pine seedlings)	1. Bowen ratio energy balance (BREB) 2. Component model	2	May-Oct	3.0	5.5	2.5
			1. Bowen ratio energy balance (BREB) 2. Component model	5	June-Sep	-0.3	4.9	6.1
			1. Bowen ratio energy balance (BREB) 2. Component model	6	June-Sep	0.9	6.1	6.8
Striegl and Wickland, 1998; Pypker and Fredeen, 2002	Saskatchewan (Canada)	Jack pine	Closed chambers	0	May-Sep	1.0	-	-
Weber, 1990; Pypker and Fredeen, 2002	Alaska (USA)	Aspen	Soda lime technique	2	year	6.2	-	-
Williams et al., 2014	Massachusetts (USA)	White and Norway spruce	Eddy covariance	0	Jun-Dec	3.2	7.6	4.4
				1	year	2.0	5.2	3.3
				2	year	1.8	5.6	3.8
Zha et al., 2009; Coursolle et al., 2012	Saskatchewan (Canada)	Jack Pine	Eddy covariance	2	year	0.4	0.7	0.3

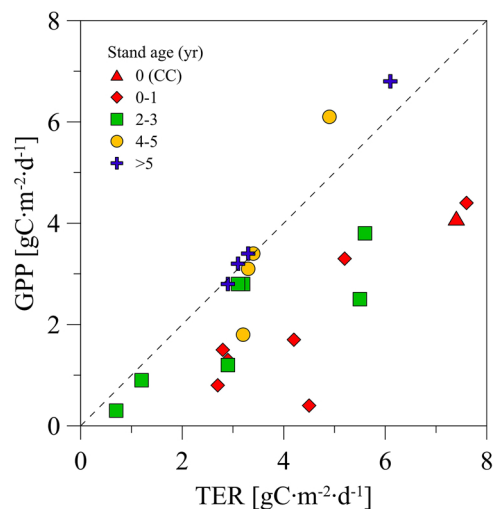


Fig. 12. Dependence between *GPP* and *TER* values for sites listed in the Table 4. Different colors and point shapes correspond to different clear-cut ages. Dashed line denotes the 1:1 line between *GPP* and *TER*.

September, data were not presented in the Table 4). Despite agreement between *NEE* rates, the *TER* and *GPP* values for these sites varied widely. In particular the *GPP* rate obtained by Paul-Limoges et al. (2015) for fresh clear-cut in Douglas fir forest were significantly lower than *GPP* at our CC site despite the higher clear-cut age.

Comparison of *NEE* estimates at CC site with  $\text{CO}_2$  flux measurements at other sites (Table 4) revealed much larger differences. A large part of these *GPP* and *TER* estimates for fresh forest clearings showed much lower *GPP* and *TER* values than the estimates for our CC site. For example, the *GPP* and *TER* of 2-year old Jack Pine clear-cut in Saskatchewan (Zha et al., 2009) didn't exceed  $0.3 \text{ gC}\cdot\text{m}^{-2}\cdot\text{d}^{-1}$  and  $0.7 \text{ gC}\cdot\text{m}^{-2}\cdot\text{d}^{-1}$  respectively. Pypker and Fredeen (2002) reported that the *GPP* of a clear-cut spruce forest in British Columbia was comparable with CC values of *GPP* around 5 years after timber harvesting ( $4.9 \text{ gC}\cdot\text{m}^{-2}\cdot\text{d}^{-1}$ ). A large diversity of *TER* and *GPP* response to clear-cutting were found for different experimental sites and can be explained by influence of numerous abiotic and biotic factors. They are varied significantly among different sites under various weather conditions, vegetation and soil properties.

It is very difficult to compare of our fluxes measurements with other experiments in the same region under similar weather, vegetation and soil conditions since there is a very sparse network of flux measurement stations in western Russia as well as total lack of such stations installed at clear-cut sites. There are  $\text{CO}_2$  fluxes data obtained by Knohl et al. (2002) at a 2-year windthrow area in a spruce-birch forest situated a few kilometers from our CC site. Measurements from July to October 1998 showed that the windthrow site was a consistent source of  $\text{CO}_2$  for the atmosphere, with *NEE* around  $2.0 \text{ gC}\cdot\text{m}^{-2}\cdot\text{d}^{-1}$ . Despite a larger amount of woody debris, *NEE* rates measured at the windthrow site were somewhat smaller than *NEE* at the CC site.

As already mentioned, the SF ecosystem, unlike the CC site, was a small sink of  $\text{CO}_2$  during the spring and the first half of summer and a source of  $\text{CO}_2$  in the late summer and autumn. Such results are consistent with previously published results of  $\text{CO}_2$  flux measurements from mature spruce forests in North America and in Europe (Falge et al., 2002; Bergeron et al., 2007; Dunn et al., 2007). Moreover, they are correlated with flux measurements in an old-growth swampy spruce forest situated within 3 km from the SF site (Kurbatova et al., 2008). Near zero  $\text{CO}_2$  balance is very typical for many boreal and sub-boreal mature forests. For example, Ueyama et al. (2014) and Soloway et al., (2017) reported that the black spruce forests in North America could be classified as a sink, source or carbon neutral depending on the period of measurements, with the carbon balance predominantly controlled by

the *TER* rate, which is highly sensitive to the temperature variations.

To analyze the processes of carbon sequestration and its release back into the atmosphere for disturbed and undisturbed forest ecosystems a relationship between *GPP* and *TER* averaged for different time intervals can be used (Fig. 12). Provided comparisons of *GPP* and *TER* rates for clear-cut areas of different ages show a clear relationship that is strongly influenced by age of forest clearing. The CC site just like the other fresh clear-cut sites is characterized by low *GPP*. The older clear-cut sites are characterized by higher *GPP* that are close to *TER* rates. The mean ratio between *GPP* and *TER* at the CC site for the growing season was about 0.55. Similar estimates were provided for clear-cuts by Humphreys et al. (2006); Kolari et al. (2004) and Williams et al. (2014). The ratio between *GPP* and *TER* obtained by Williams et al. (2014) during the experimental study in the white and Norway spruce forest during the first year following harvest in Massachusetts was 0.58 and this value was the closest point to our CC site that is presented in Fig. 12. As reported by Amiro et al. (2010), the ratio of *GPP* to *TER* varied between 0.2 and 1.2 at most post-harvest sites in North America during the first 10–20 years after the disturbance.

Kowalski et al. (2003) provided comparisons of *GPP* and *TER* for clear-cut and undisturbed forest stand and showed that while the ratio for fresh clear-cut was about 0.7, the ratio for mature forests was about 1.3. Paul-Limoges et al. (2015) observed extremely large differences in *GPP*: *TER* between mature and harvested sites in Douglas fir forest: the ratio was 1.4 for the mature forest and 0.01 for the clear-cut. Falge et al. (2002) summarized numerous available eddy-covariance data and showed that the ratio between *GPP* and *TER* in summer for the most undisturbed boreal dark coniferous forests in central and northern Europe can range between 1.2 and 2.0 and between 1.1 and 2.3 for deciduous temperate forests. The *GPP* and *TER* ratio for our SF site was 0.98 and it is some lower than the range defined by Falge et al. (2002). The main reasons of such dependence can be decreased *GPP* of old-age unmanaged forest stand as well as high *TER* rates influenced particularly by high heterotrophic respiration rates.

Estimating the contribution of different ecosystem components (e.g. autotrophic and heterotrophic soil respiration, respiration of above ground grassy and woody vegetation, respiration of woody residuals, etc.) to total *TER* was beyond the scope of our current study. However, taking into account the possible strong influence of heterotrophic respiration on total *TER* both at CC area during the first years after the timber harvest and at SF site we quantify it using the simple empirical approach that is broadly used in experimental studies (Amiro et al., 2010; Jassal et al., 2007; Landsberg and Waring, 1997):

$$R_{het} = TER - 0.55 \cdot GPP \quad (6)$$

According to this assumption the fraction of heterotrophic respiration in SF site reached 46% of *TER* ( $3.25 \text{ gC}\cdot\text{m}^{-2}\cdot\text{d}^{-1}$ ) while at CC site it was about 70% of *TER* ( $5.15 \text{ gC}\cdot\text{m}^{-2}\cdot\text{d}^{-1}$ ) during the growing season. Such simple estimates actually agreed well with results of the field experiments provided by Gao et al. (2015) and Paul-Limoges et al. (2015), which showed that clear-cutting can reduce autotrophic respiration and *TER* by 15 and 16%, respectively. It can be expected that during the spring before the beginning of active vegetation growth the heterotrophic respiration at CC site could be significantly higher than the respiration at SF site. In the second half of summer due to active vegetation recovery at CC site the fractions of autotrophic respiration in *TER* can be drastically increased.

#### 4.3. The dependencies of the $\text{CO}_2$ fluxes on environmental parameters

The field measurements showed that the *TER* variability at both experimental sites is mainly influenced by the air temperature variation. It is important to note that  $Q_{10}$  calculated using the air temperature data at SF and CC sites did not significantly differ (2.64 for SF and 2.21 for CC site, respectively), and they are comparable with estimations obtained in some other studies. For example, the  $Q_{10}$  values estimated in a 2 year clear-cut black spruce stand in Quebec was about

2.20 (Giasson et al., 2006). Bergeron et al. (2008) also reported that differences in  $Q_{10}$  between mature black spruce forest and 4-year clear-cut were not very different (2.6 in the old-age stand and 2.8 - at the harvested one). On the other hand the  $Q_{10}$  values obtained using the soil temperature data are differed from  $Q_{10}$  estimates provided using air temperature data and they are some higher. The different shapes of temperature response curves for  $TER$  estimates based on the air or soil temperatures resulted in different estimates of  $R_{10}$  values. Whereas  $R_{10}$  estimated from the air temperatures for CC site was quite similar to SF site, the  $R_{10}$  estimated from the soil temperatures for CC site was about 30% lower than at SF site. Similar responses of  $R_{10}$  to soil temperature changes was reported by Mkhabela et al. (2009) from 2-year measurements in a mature Jack Pine forest and in 10 and 2-year clear cuts in Saskatchewan. Results showed that the mature forest stand is characterized by highest  $R_{10}$  values, and the cleared areas by the lowest ones. The strong inter-annual variation of  $Q_{10}$  as well as the dependence between  $Q_{10}$  values and clear-cut age was also detected.

Comparisons of photosynthetic light use efficiency values for CC and SF sites showed that the CC site was characterized by higher  $\epsilon$  than SF. The similar result for non-disturbed and harvested forest ecosystems were provided by Paul-Limoges et al. (2015). Under low daily PAR values which are smaller than  $10\text{--}15 \text{ mol m}^{-2} \text{ d}^{-1}$  (e.g. for periods with cloudy weather conditions) mainly due to a non-linear shape of the light response curves for SF site the difference between  $\epsilon$  for SF and CC sites are insignificant. The strong response of  $GPP$  at CC site to incoming PAR could be an important factors determining the relatively high  $GPP$  at CC site during the first year after timber harvesting. The light saturation for the CC site was reached under the lower PAR values (approximately at  $600 \mu\text{mol m}^{-2} \text{ s}^{-1}$  of PAR) in comparison with SF site. The same value was obtained for the clear-cuts in Black spruce and Scots pine forests by Giasson et al. (2006) and Kolari et al. (2004), respectively. It should be noted that the dependence of  $GPP$  on PAR was obtained for relatively warm and wet weather conditions of the year 2016. It can be expected that additional experimental data for the area covering larger spectrum of weather conditions including the air and soil temperature patterns, as well as soil moisture condition can make the relationships between  $GPP$  and PAR more accurate and precise.

## 5. Conclusions

The results of meteorological and eddy covariance flux measurements conducted in an undisturbed mature spruce forest and at a clear-cut site during the first growing season following timber harvest in the South-European taiga forest showed that the clear-cutting can strongly influence the radiation, energy and  $\text{CO}_2$  fluxes between the land surface and atmosphere.

The CC site was characterized by higher albedo (up to 25%) and reduced mean net radiation in comparison with undisturbed mature SF. Daily sums of  $H$  and  $LE$  fluxes at the CC were lower by 22 and 48%, respectively, whereas  $G$  amplitude was higher by 32% in comparison with SF site. Seasonal patterns of different energy balance components at both sites were quite similar and characterized by higher  $H$  during spring and early summer with mean daily  $\beta$  close to 1 and by higher  $LE$  rates in the second half of summer and in early autumn with  $\beta$  that are consistently less than 1. The mean  $\beta$  for the entire measurement period was quite the same ( $\beta \approx 0.5$ ) at both sites. Effect of forest clearing on  $\text{CO}_2$  fluxes were also evident. There was a sharp decline in  $GPP$  after timber harvest despite active vegetation recovery within the clear-cut during the summer. On the other hand, there was little change in daily  $TER$ , which resulted in sustained losses of carbon from the forested lands: whereas average  $NEE$  at the undisturbed mature forest was close to zero, daily  $NEE$  at the clear-cut was always positive ( $3.3 \pm 1.3 \text{ gC}\cdot\text{m}^{-2}\cdot\text{d}^{-1}$ ; carbon source).

Comparisons of our flux measurements with observations previously conducted at other sites of boreal forest zone showed a large diversity of possible responses of atmospheric fluxes to forest disturbances. The

variety of responses is influenced by different abiotic and biotic factors e.g. forest types, local weather and climatic conditions, soil properties, silviculture and timber harvesting methods. To clarify the features and the reasons of possible differences in responses of various forest ecosystems the new data for more accurate and multifaceted analysis of  $\text{CO}_2$ , water vapor and energy fluxes at disturbed ecosystems based on both experimental and modeling studies are very necessary. The various process-based atmospheric models in this case - can be used to better understand key mechanisms of the land surface - atmosphere interaction and project the effects of forest disturbances on atmospheric conditions on local and regional scales. Such aggregated studies are especially important taking into account a high deforestation rate observed in European part of Russia during the last decades and projected growth of human impacts on the forest ecosystems in the region. Taking into account the strong influence of forest disturbance on local radiation, energy and  $\text{CO}_2$  fluxes the significant changes of regional atmospheric conditions (e.g. air temperature, humidity, precipitation, cloudiness) due to deforestation processes caused by e.g. clear-cut harvesting, are very likely.

## Acknowledgements

The flux measurements at the clear-cut site and data post processing provided by Mamkin V., Ivanov D., Olchev A. and Kurbatova J. were supported by the grant of the Russian Science Foundation (14-14-00956). Field study conducted by Avilov V., Kuricheva O. and Varlagin A. in an undisturbed spruce forest were supported by the grants of the Russian Foundation for Basic Research and the Russian Geographical Society (projects: 16-04-01754 A and 17-05-41127) and partially by the grant of the Presidium of the Russian Academy of Sciences, program № 41 “Biodiversity of natural systems and biological resources of Russia”. We thank Logan Berner from EcoSpatial Services L.L.C. (USA) for fruitful comments and English edits on the manuscript.

## References

- Aguilos, M., Takagi, K., Liang, N., Ueyama, M., Fukuzawa, K., Nomura, M., Kishida, O., Fukuzawa, T., Takahashi, H., Kotsuka, C., Sakai, R., Ito, K., Watanabe, Y., Fujinuma, Y., Takahashi, Y., Muragama, T., Saigusa, N., Sakai, R., 2014. Dynamics of ecosystem carbon balance recovering from a clear-cutting in a cool-temperate forest. *Agric. For. Meteorol.* 197, 26–39.
- Amiro, B.D., 2001. Paired-tower measurements of carbon and energy fluxes following disturbance in the boreal forest. *Glob. Change Biol.* 7, 253–268.
- Amiro, B.D., Barr, A.G., Black, T.A., Iwashita, H., Kljun, N., McCaughey, J.H., Morgenstern, K., Murayama, S., Nesic, Z., Orchansky, A.L., Saigusa, N., 2006. Carbon, energy and water fluxes at mature and disturbed forest sites, Saskatchewan, Canada. *Agric. For. Meteorol.* 136, 237–251.
- Amiro, B.D., Barr, A.G., Barr, J.G., Black, T.A., Bracho, R., Brown, M., Chen, J., Clark, K.L., Davis, K.J., Desai, A.R., Dore, S., Engel, V., Fuentes, J.D., Goldstein, A.H., Goulden, M.L., Kolb, T.E., Lavigne, M.B., Law, B.E., Margolis, H.A., Martin, T., McCaughey, J.H., Misson, L., Montes-Helu, M., Noormets, A., Randerson, J.T., Starr, G., Xiao, J., 2010. Ecosystem carbon dioxide fluxes after disturbance in forests of North America. *J. Geophys. Res.* 115, G00K02.
- Aubinet, M., Vesala, T., Papale, D., 2012. *Eddy Covariance: A Practical Guide to Measurement and Data Analysis*. Springer, Dordrecht, The Netherlands, pp. 438.
- Bergeron, O., Margolis, H.A., Coursolle, C., Giasson, M.A., 2008. How does forest harvest influence carbon dioxide fluxes of black spruce ecosystems in eastern North America? *Agric. For. Meteorol.* 148 (4), 537–548.
- Burba, G., 2013. Eddy covariance method for scientific, industrial, agricultural and regulatory applications: a field book on measuring ecosystem gas exchange and areal emission rates. *LI-Cor Biosci.* 332.
- Carlson, D.W., Groot, A., 1997. Microclimate of clearcut, forest interior, and small openings in trembling aspen forest. *Agric. For. Met.* 87, 313–329.
- Cherubini, F., Bright, R.M., Strømman, A.H., 2012. Site-specific global warming potentials of biogenic  $\text{CO}_2$  for bioenergy: contributions from carbon fluxes and albedo dynamics. *Environ. Res. Lett.* 7 (4), 045902.
- Chen, H.Y.H., Luo, Y., 2015. Net aboveground biomass declines of four major forest types with forest ageing and climate change in western Canada's boreal forests. *Glob. Change Biol.* 21 (10), 3675–3684.
- Coursolle, C., Margolis, H.A., Giasson, M.A., Bernier, P.Y., Amiro, B.D., Arain, M.A., Barr, A.G., Black, T.A., Goulden, M.L., McCaughey, J.H., Chen, J.M., Dunn, A.L., Grant, R.F., Lafleur, P.M., 2012. Influence of stand age on the magnitude and seasonality of carbon fluxes in Canadian forests. *Agric. For. Meteorol.* 165, 136–148.
- Desherevskaya, O., Kurbatova, J., Olchev, A., 2010. Climatic conditions of the south part of Valdai hills, Russia, and their projected changes during the 21st century. *Open*

- Geogr. J. 3, 73–79.
- Dunn, A.L., Barford, C.C., Wofsy, S.C., Goulden, M.L., Daube, B.C., 2007. A long-term record of carbon exchange in a boreal black spruce forest: means, responses to inter-annual variability, and decadal trends. *Glob. Change Biol.* 13 (3), 577–590.
- Falge, E., Baldocchi, D., Tenhunen, J., Aubinet, M., Bakwin, P., Berbigier, P., Bernhofer, C., Burba, G., Clement, R., Davis, K.J., Elbers, J.A., Goldstein, A.H., Grelle, A., Granier, A., Guðmundsson, J., Hollinger, D., Kowalski, A.S., Katul, G., Law, B.E., Malhi, Y., Meyers, T., Monson, R.K., Munger, J.T., Oechel, W., Paw, K.T.U., Pilegaard, K., Rannik, Ü., Rebmann, C., Suyker, A., Valentini, R., Wilson, K., Wofsy, S., 2002. Seasonality of ecosystem respiration and gross primary production as derived from FLUXNET measurements. *Agric. For. Meteorol.* 113 (1), 53–74.
- Falge, E., Reth, S., Brüggemann, N., Butterbach-Bahl, K., Goldberg, V., Oltchev, A., Schaaf, S., Spindler, G., Stiller, B., Queck, R., Köstner, B., Bernhofer, C., 2005. Comparison of surface energy exchange models with eddy flux data in forest and grassland ecosystems of Germany. *Ecol. Modell.* 188, 174–216.
- FAO, 2011. *State of the World's Forests 2011*. Rome, pp. 179. [www.fao.org/docrep/013/i2000e/i2000e00.htm](http://www.fao.org/docrep/013/i2000e/i2000e00.htm).
- Fernandez, L.J., Son, Y., Kraske, C.R., Rustad, L.E., David, M.B., 1993. Soil carbon dioxide characteristics under different forest types and after harvest. *Soil Sci. Soc. Am. J.* 57, 1115–1121.
- Gao, S., Chen, J., Tang, Y., Xie, J., Zhang, R., Tang, J., Zhang, X., 2015. Ecosystem carbon (CO<sub>2</sub> and CH<sub>4</sub>) fluxes of a Populus deltoides plantation in subtropical China during and post clear-cutting. *For. Ecol. Manage.* 357, 206–219.
- Garrett, L.G., Kimberley, M.O., Oliver, G.R., Pearce, S.H., Beets, P.N., 2012. Decomposition of coarse woody roots and branches in managed Pinus radiata plantations in New Zealand: a time series approach. *For. Ecol. Manage.* 269, 116–123.
- Giasson, M.A., Coursolle, C., Margolis, H.A., 2006. Ecosystem-level CO<sub>2</sub> fluxes from a boreal cutover in eastern Canada before and after scarification. *Agric. For. Meteorol.* 140 (1–4), 23–40.
- Gordon, A.M., Schlentner, R.E., Van Cleve, K., 1987. Seasonal patterns of soil respiration and CO<sub>2</sub> evolution following harvesting in the white spruce forests of interior Alaska. *Can. J. For. Res.* 17, 304–310.
- Grant, R.F., Barr, A.G., Black, T.A., Margolis, H.A., McCaughey, J.H., Trofymow, J.A., 2010. Net ecosystem productivity of temperate and boreal forests after clearcutting - a fluxnet-Canada measurement and modelling synthesis. *Tellus Ser. B* 62 (5), 475–496.
- Hashimoto, S., 2005. Q 10 values of soil respiration in Japanese forests. *J. For. Res.* 10, 409–413.
- Helbig, M., Chasmer, L.E., Desai, A.R., Kljun, N., Quinton, W.L., Sonntag, O., 2017. Direct and indirect climate change effects on carbon dioxide fluxes in a thawing boreal forest-wetland landscape. *Glob. Change Biol.* 23 (8), 3231–3248.
- Hirata, R., Takagi, K., Ito, A., Hirano, T., Saigusa, N., 2014. The impact of climate variation and disturbances on the carbon balance of forests in Hokkaido, Japan. *Biogeosciences* 11 (18), 5139.
- Humphreys, E.R., Black, T.A., Morgenstern, K., Cai, T., Drewitt, G.B., Nesic, Z., Trofymow, J.A., 2006. Carbon dioxide fluxes in coastal Douglas-fir stands at different stages of development after clearcut harvesting. *Agric. For. Meteorol.* 140 (1–4), 6–22.
- Ivanov, D.G., Avilov, V.K., Kurbatova, Y.A., 2017. CO<sub>2</sub> fluxes at south taiga bog in the European part of Russia in summer. *Contemp. Prob. Ecol.* 10 (2), 97–104.
- IPCC, 2013. *Climate Change 2013: The Physical Science Basis*. Cambridge University Press, Cambridge, United Kingdom and New York, NY, USA, pp. 1535.
- Jassal, R.S., Black, T.A., Cai, T., Morgenstern, K., Li, Z., Gaumont Guay, D., Nesic, Z., 2007. Components of ecosystem respiration and an estimate of net primary productivity of an intermediate-aged Douglas-fir stand. *Agric. For. Meteorol.* 144, 44–57.
- Keenan, R.J., Kimmins, J.P., 1993. The ecological effects of clear-cutting. *Environ. Rev.* 1 (2), 121–144.
- Knohl, A., Kolle, O., Minayeva, T.Y., Milyukova, I.M., Vygodskaya, N.N., Foken, T., Schulze, E.D., 2002. Carbon dioxide exchange of a Russian boreal forest after disturbance by wind throw. *Glob. Change Biol.* 8 (3), 231–246.
- Kljun, N., Calanca, P., Rotach, M.W., Schmid, H.P., 2004. A simple parameterisation for flux footprint predictions. *Boundary Layer Meteorol.* 112, 503–523.
- Kolari, P., Pumpanen, J., Rannik, Ü., Ilvesniemi, H., Hari, P., Berninger, F., 2004. Carbon balance of different aged Scots pine forests in Southern Finland. *Glob. Change Biol.* 10 (7), 1106–1119.
- Kowalski, S., Sartore, M., Burlett, R., Berbigier, P., Loustau, D., 2003. The annual carbon budget of a French pine forest (Pinus pinaster) following harvest. *Glob. Change Biol.* 9 (7), 1051–1065.
- Kuricheva, O., Mamkin, V., Sandlersky, R., Puzachenko, J., Varlagin, A., Kurbatova, J., 2017. Radiative entropy production along the paludification gradient in the Southern Taiga. *Entropy* 19 (1), 43.
- Kulmala, L., Aaltonen, H., Berninger, F., Kielloaho, A.J., Levula, J., Bäck, J., Hari, P., Kolari, P., Korhonen, J.F.J., Kulmala, M., Nikinmaa, E., Pihlatie, M., Vesala, T., Pumpanen, J., 2014. Changes in biogeochemistry and carbon fluxes in a boreal forest after the clear-cutting and partial burning of slash. *Agric. For. Meteorol.* 188, 33–44.
- Kurbatova, J., Li, C., Varlagin, A., Xiao, X., Vygodskaya, N., 2008. Modeling carbon dynamics in two adjacent spruce forests with different soil conditions in Russia. *Biogeosciences* 5, 969–980.
- Kuzmina, E.V., Oltchev, A.V., Rozinkina, I.A., Rivin, G.S., Nikitin, M.A., 2017. Application of the COSMO-CLM mesoscale model to assess the effects of forest cover changes on regional weather conditions in the European part of Russia. *Russ. Meteorol. Hydrol.* 42 (9), 574–581.
- Landsberg, J.L., Waring, R.H., 1997. A generalised model of forest productivity using simplified concepts of radiation-use efficiency, carbon balance and partitioning. *For. Ecol. Manage.* 95, 209–228.
- Lasslop, G., Reichstein, M., Papale, D., Richardson, A.D., Arneeth, A., Barr, A., Stoy, P., Wohlfahrt, G., 2010. Separation of net ecosystem exchange into assimilation and respiration using a light response curve approach: critical issues and global evaluation. *Glob. Change Biol.* 16 (1), 187–208.
- Lloyd, J., Taylor, Ya., 1994. On the temperature dependence of soil respiration. *Func. Ecol.* 8 (3), 315–323.
- Lyons, E.A., Jin, Y., Randerson, J.T., 2008. Changes in surface albedo after fire in boreal forest ecosystems of interior Alaska assessed using MODIS satellite observations. *J. Geophys. Res. Biogeosci.* 113.
- Lytle, D.E., Cronan, C.S., 1998. Comparative soil CO<sub>2</sub> evolution, litter decay, and root dynamics in clearcut and uncut spruce-fir forest. *For. Ecol. Manage.* 103 (2–3), 121–128.
- Machimura, T., Kobayashi, Y., Hirano, T., Lopez, L., Fukuda, M., Fedorov, A.N., 2005. Change of carbon dioxide budget during three years after deforestation in eastern Siberian larch forest. *J. Agric. Meteorol.* 60 (5), 653–656.
- Mamkin, V., Kurbatova, J., Avilov, V., Mukhartova, Y., Krupenko, A., Ivanov, D., Levashova, N., Oltchev, A., 2016. Changes in net ecosystem exchange of CO<sub>2</sub>, latent and sensible heat fluxes in a recently clear-cut spruce forest in western Russia: results from an experimental and modeling analysis. *Environ. Res. Lett.* 11 (12), 125012.
- Matthews, B., Mayer, M., Katzensteiner, K., Godbold, D.L., Schume, H., 2017. Turbulent energy and carbon dioxide exchange along an early-successional windthrow chronosequence in the European Alps. *Agric. For. Meteorol.* 232 (15), 576–594.
- Mauder, M., Foken, T., 2006. Impact of post-field data processing on eddy covariance flux estimates and energy balance closure. *Meteorol. Z.* 15, 597–609.
- McCaughey, J.H., 1985. A radiation and energy balance study of mature forest and clear-cut sites. *Boundary-Layer Meteorol.* 32, 1–24.
- McCaughey, J.H., 1987. The albedo of a mature mixed forest and a clear-cut site at Petawawa, Ontario. *Agric. For. Meteorol.* 40 (3), 251–263.
- Migliavacca, M., Meroni, M., Manca, G., Matteucci, G., Montagnani, L., Grassi, G., Zenone, T., Teobaldelli, M., Godeed, L., Colombo, R., Seufert, G., 2009. Seasonal and interannual patterns of carbon and water fluxes of a poplar plantation under peculiar eco-climatic conditions. *Agric. For. Meteorol.* 149, 1460–1476.
- Mkhabela, M.S., Amiro, B.D., Barr, A.G., Black, T.A., Hawthorne, I., Kidston, J., McCaughey, J.H., Orchansky, A.L., Nesic, Z., Sass, A., Shashkov, A., Zha, T., 2009. Comparison of carbon dynamics and water use efficiency following fire and harvesting in Canadian boreal forests. *Agric. For. Meteorol.* 149 (5), 783–794.
- Molchanov, A.G., Kurbatova, Yu.A., Oltchev, A.V., 2017. Effect of clear-cutting on soil CO<sub>2</sub> emission. *Biol. Bull.* 44 (2), 218–223.
- Monsi, M., Saeki, T., 1953. Ueber den Lichtfaktor in den Pflanzengesellschaften und seine Bedeutung für die Stoffproduktion. *Jpn. J. Bot.* 14, 22–52.
- Monteith, J.L., 1977. Climate and the efficiency of crop production in Britain. *Philos. Trans. R. Soc. Lond. B* 281, 277–294.
- Mukhartova, Yu.V., Levashova, N.T., Oltchev, A.V., Shapkina, N.E., 2015. Application of a 2D model for describing the turbulent transfer of CO<sub>2</sub> in a spatially heterogeneous vegetation cover. *Moscow Univ. Phys. Bull.* 70 (1), 14–21.
- Novenko, E., Tsyganov, A.N., Oltchev, A.V., 2018. Palaeoecological data as a tool to predict possible future vegetation changes in the boreal forest zone of European Russia: a case study from the Central Forest Biosphere Reserve. *IOP Conf. Series: Earth Environ. Sci.* 107, 012104.
- Oltchev, A., Cermak, J., Nadezhdina, N., Tatarinov, F., Tishenko, A., Ibrom, A., Gravenhorst, G., 2002. Transpiration of a mixed forest stand: field measurements and simulation using SVAT models. *Boreal Environ. Res.* 7 (4), 389–397.
- Oltchev, A.V., Mukhartova, Yu.V., Levashova, N.T., Volkova, E.M., Ryzhova, M.S., Mangura, P.A., 2017. The influence of the spatial heterogeneity of vegetation cover and surface topography on vertical CO<sub>2</sub> fluxes within the atmospheric surface layer. *Izv., Atmos. Oceanic Phys.* 53 (5), 539–549.
- Oltchev, A., Radler, K., Sogachev, A., Panferov, O., Gravenhorst, G., 2009. Application of a three-dimensional model for assessing effects of small clear-cuttings on radiation and soil temperature. *Ecol. Modell.* 220 (21), 3046–3056.
- Oltchev, A.V., Rozinkina, I.A., Kuzmina, E.V., Nikitin, M.A., Rivin, G.S., 2018. Influence of forest cover changes on regional weather conditions: estimations using the mesoscale model COSMO. *IOP Conf. Series: Earth Environ. Sci.* 107, 012105.
- Panferov, O., Sogachev, A., 2008. Influence of gap size on wind damage variables in a forest. *Agric. For. Meteorol.* 148, 1869–1881.
- Papale, D., Reichstein, M., Aubinet, M., Canfora, E., Bernhofer, C., Kutsch, W., Longdoz, B., Rambal, S., Valentini, R., Vesala, T., Yakir, D., 2006. Towards a standardized processing of net ecosystem exchange measured with eddy covariance technique: algorithms and uncertainty estimation. *Biogeosciences* 3 (4), 571–583.
- Paul-Limoges, E., Black, T.A., Christen, A., Nesic, Z., Jassal, R.S., 2015. Effect of clearcut harvesting on the carbon balance of a Douglas-fir forest. *Agric. For. Meteorol.* 203, 30–42.
- Pavelka, M., Acosta, M., Marek, M.V., Kutsch, W., Janous, D., 2007. Dependence of the Q10 values on the depth of the soil temperature measuring point. *Plant Soil* 292 (1–2), 171–179.
- Peel, M.C., Finlayson, B.L., McMahon, T.A., 2007. Updated world map of the Köppen-Geiger climate classification. *Hydrol. Earth Syst. Sci.* 11, 1633–1644.
- Pypker, T.G., Fredeen, A.L., 2002. Ecosystem CO<sub>2</sub> flux over two growing seasons for a sub-boreal clearcut 5 and 6 years after harvest. *Agric. For. Meteorol.* 114 (1–2), 15–30.
- Radler, K., Oltchev, A., Panferov, O., Klinck, U., Gravenhorst, G., 2010. Radiation and temperature responses to a small clear-cut in a spruce forest. *Open Geogr. J.* 3, 103–114.
- Rannik, Ü., Altimir, N., Raittila, J., Suni, T., Gaman, A., Hussein, T., Hölttä, T., Lassila, H., Latokartano, M., Lauri, A., Natsheh, A., Petäjä, T., Storaajama, R., Yiä-Mella, H., Keronen, P., Berninger, F., Vesala, T., Hari, P., Kulmala, M., 2002. Fluxes of carbon dioxide and water vapour over Scots pine forest and clearing. *Agric. For. Meteorol.* 111 (3), 187–202.
- Reichstein, M., Falge, E., Baldocchi, D., Papale, D., Aubinet, M., Berbigier, P., Bernhofer,

- C., Buchmann, N., Gilmanov, T., Granier, A., Grünwald, T., Harránková, K., Ilvesniemi, H., Janous, D., Knohl, A., Laurila, T., Lohila, A., Loustau, D., Matteucci, G., Meyers, T., Miglietta, F., Ourcival, J.-M., Pumpanen, J., Rambal, S., Rotenberg, E., Sanz, M., Tenhunen, J., Seufert, G., Vaccari, F., Vesala, T., Yakir, D., Valentini, R., 2005. On the separation of net ecosystem exchange into assimilation and ecosystem respiration: review and improved algorithm. *Global Change Biol.* 11 (9), 1424–1439.
- Richardson, A.D., Braswell, B.H., Hollinger, D.Y., Burman, P., Davidson, E.A., Evans, R.S., Flangan, L.B., Munger, J.W., Savage, K., Urbanski, S., Wofsy, S.C., 2006. Comparing simple respiration models for eddy flux and dynamic chamber data. *Agric. For. Meteorol.* 141 (2–4), 219–234.
- Rosati, A., Metcalf, S.G., Lampinen, B.D., 2004. A simple method to estimate photosynthetic radiation use efficiency of canopies. *Ann. Bot.* 93, 567–574.
- Schulze, E.D., Wirth, C., Heimann, M., 2000. Managing forests after Kyoto. *Science* 289 (5487), 2058–2059.
- Seidl, R., Schelhaas, M.J., Rammer, W., Verkerk, P.J., 2014. Increasing forest disturbances in Europe and their impact on carbon storage. *Nat. Clim. Change* 4 (9), 806.
- Soloway, A.D., Amiro, B.D., Dunn, A.L., Wofsy, S.C., 2017. Carbon neutral or a sink? Uncertainty caused by gap-filling long-term flux measurements for an old-growth boreal black spruce forest. *Agric. For. Meteorol.* 233, 110–121.
- Striegl, R.G., Wickland, K.P., 1998. Effects of a clear-cut harvest on respiration in a jack pine-lichen woodland. *Can. J. For. Res.* 28, 534–539.
- Sundqvist, E., Vestin, P., Crill, P., Persson, T., Lindroth, A., 2014. Short-term effects of thinning, clear-cutting and stump harvesting on methane exchange in a boreal forest. *Biogeosciences* 11, 6095–6105.
- Tzwang, L.R., Koprof, B.M., Zubkonskii, S.L., Dyer, A.J., Hisks, B.B., Hisks, B.B., Miyake, M., Stewart, R.W., McDonald, J.W., 1973. A comparison of turbulence measurements by different instruments: Tsimlyansk field experiment. *Boundary-Layer Meteorol.* 3, 499–521.
- Twine, T.E., Kustas, W.P., Norman, J.M., Cook, D.R., Houser, P.R., Meyers, T.P., Prueger, J.H., Starks, P.J., Wesely, M.L., 2000. Correcting eddy-covariance flux underestimates over a grassland. *Agric. For. Meteorol.* 103, 279–300.
- Ueyama, M., Iwata, H., Harazono, Y., 2014. Autumn warming reduces the CO<sub>2</sub> sink of a black spruce forest in interior Alaska based on a nine-year eddy covariance measurement. *Glob. Change Biol.* 20 (4), 1161–1173.
- Weber, M.G., 1990. Forest soil respiration after cutting and burning in immature aspen ecosystems. *For. Ecol. Manage.* 31, 1–14.
- Williams, C.A., Vanderhoof, M.K., Khomik, M., Ghimire, B., 2014. Post-clearcut dynamics of carbon, water and energy exchanges in a midlatitude temperate, deciduous broadleaf forest environment. *Glob. Change Biol.* 20 (3), 992–1007.
- Willmott, C.J., Feddema, J.J., 1992. A more rational climatic moisture index. *Prof. Geogr.* 44, 84–88.
- Wilson, K., Goldstein, A., Falge, E., Aubinet, M., Baldocchi, D., Berbigier, P., Bernhofer, Ceulemans, R., Dolman, H., Field, C., Grelle, A., Ibrom, A., Law, B.E., Kowalski, A., Meyers, T., Moncrieff, J., Monson, R., Oechel, W., Tenhunen, J., Valentini, R., Verma, S., 2002. Energy balance closure at FLUXNET sites. *Agric. For. Meteorol.* 113 (1), 223–243.
- Wutzler, T., Lucas-Moffat, A., Migliavacca, M., Knauer, J., Sickel, K., Šigut, L., Menzer, O., Reichstein, M., 2018. Basic and extensible post-processing of eddy covariance flux data with REddyProc. *Biogeosciences* 15, 5015–5030. <https://doi.org/10.5194/bg-15-5015-2018>.
- Zamolodchikov, D.G., Grabovskii, V.I., Shulyak, P.P., Chestnykh, O.V., 2017. Recent decrease in carbon sink to Russian forests. *Doklady Biol. Sci.* 476 (1), 200–202.
- Zha, T., Barr, A.G., Black, T., McCaughey, J.H., Bhatti, J., Hawthorne, I., Nestic, Z., 2009. Carbon sequestration in boreal jack pine stands following harvesting. *Glob. Change Biol.* 15 (6), 1475–1487.